NAVAL SHIP RESEARCH AND DEVELOPMENT CENTER
WASHINGTON, D.C. 20007

COMPARISONS OF EXPERIMENTALLY DETERMINED AND THEORETICALLY PREDICTED PRESSURES IN THE VICINITY OF A MARINE PROPELLER

by

Stephen B. Denny

HYDROMECHANICS LABORATORY
RESEARCH AND DEVELOPMENT REPORT

May 1967 Report 2349

COMPARISONS OF EXPERIMENTALLY DETERMINED AND THEORETICALLY PREDICTED PRESSURES IN THE VICINITY OF A MARINE PROPELLER Report 2349

The Naval Ship Research and Development Center is a U.S. Navy center for laboratory effort directed at achieving improved sea and air vehicles. It was formed in March 1967 by merging the David Taylor Model Basin at Carderock, Maryland and the Marine Engineering Laboratory at Annapolis, Maryland.

Naval Ship Research and Development Center
Washington, D. C. 20007

COMPARISONS OF EXPERIMENTALLY DETERMINED AND THEORETICALLY PREDICTED PRESSURES IN THE VICINITY OF A MARINE PROPELLER

by

Stephen B. Denny

May 1967

Report 2349
Z-R011 01 01

TABLE OF CONTENTS

LIST OF FIGURES

Page

Page

Page

NOTATION

a_n	Fourier cosine coefficient of the blade-rate harmonic of the pressure signal
b_n	Fourier sine coefficient of the blade-rate harmonic of the pressure signal
$C(\eta)$	Amplitude of the ηth harmonic of the circumferentially varying wake
c_n	Amplitude of the blade-rate pressure signal, $c_n = [(a_n)^2 + (b_n)^2]^{1/2}$
D	Propeller diameter
$E.A.R.$	Propeller expanded area ratio
f	Blade section camber
G	Nondimensional total bound circulation of propeller, $G = \frac{\Gamma}{\pi DV}$
J	Advance coefficient, $J = \frac{V}{ND}$
K_p	Nondimensional pressure coefficient, $K_p = \frac{\Delta p}{\rho N^2 D^2}$
K_{p_n}	Nondimensional blade-rate pressure coefficient
$(K_p)_t$	Thickness contribution pressure coefficient
$(K_p)_\Gamma$	Loading contribution pressure coefficient
K_Q	Torque coefficient, $K_Q = \frac{Q}{\rho N^2 D^5}$
K_T	Thrust coefficient, $K_T = \frac{T}{\rho N^2 D^4}$
ℓ	Blade section length
N	Propeller revolutions per second

n	Number of blades
P	Blade section pitch
Δp	Pressure amplitude
R	Propeller radius
r	Radial distance from the propeller axis
t	Maximum thickness of propeller blade section
V	Speed of advance
$\overline{V}$	Volume mean flow velocity downstream of wake screen
$\overline{V}_\eta$	Ratio of the amplitude of the ηth wake harmonic to the volume mean flow velocity
x	Axial distance from the propeller plane
β	Advance angle
β_i	Hydrodynamic pitch angle
Γ	Total bound circulation
γ	Dummy phase angle
η	Harmonic number in wake analysis
θ	Phase angle of maximum induced blade-rate pressure, $\theta = \frac{1}{n}\tan^{-1}\left(\frac{b_n}{a_n}\right)$
ρ	Density of fluid
σ	Cavitation number, $\sigma = \frac{2gH}{V^2}$
ϕ	Rotative angle between the blade centerline and the projection of the field point into the propeller plane
ϕ_η	Phase angle of the ηth harmonic of the wake
ω	Angular velocity, $\omega = 2\pi N$

ABSTRACT

Pressures were measured on a flat plate placed near a model marine propeller in the 24-inch water tunnel at the David Taylor Model Basin. The blade-rate portions of the values measured in uniform flow are compared with field-point pressure predictions of theories for two propeller tip clearances and three advance conditions. Also shown are comparisons between theory and experiment of the separate contributions of propeller thickness and loading.

Additional experimental results show the effect of blade number, blade area ratio, and blade skew on propeller-induced pressures. Flat-plate pressure measurements were also obtained near a propeller operating in nonuniform flow and at a cavitating condition in uniform flow.

The two theories investigated, field-point pressure calculation methods by Kerwin and by Breslin, both gave good predictions of the magnitudes of the induced blade-rate pressures due to blade thickness. The experimentally determined blade-rate pressures due to loading and the consequent total pressures, however, tended to be lower than the theoretical predictions downstream of the propeller. Breslin's theory gave predictions of pressure phase which were poor for the entire experimental region, whereas the predictions of Kerwin's method were good except in the aforementioned downstream area.

From the experiments it was found that a considerable reduction in induced blade-rate pressure results from increased blade area and extreme blade skew. Propeller blade cavitation increased the induced field pressures. Pressures induced by the propeller while it operated in nonuniform flow tended to be considerably larger than those induced during a corresponding advance in uniform flow and particularly so at off-design advance conditions.

ADMINISTRATIVE INFORMATION

This work was performed at the David Taylor Model Basin under Bureau of Ships Subproject Z-R011 01 01, Problem Number 526-356.

INTRODUCTION

In recent years several investigators have been involved in experimental studies of marine propeller induced pressures. In 1957 Tachmindji and Dickerson[1] presented results of free-space pressure measurements obtained near a propeller operating in the 12-inch water

[1]References are listed on page 42.

tunnel at the David Taylor Model Basin. Their work explored the effects of propeller rpm, advance, number of blades, in addition to the effect of varying the horizontal, vertical, and transverse location of the measuring transducer.

In 1960 Pohl[2] published the results of measurements he had made on a flat plate near propellers operating in a free-surface water channel at the Hamburg Model Basin. His extensive testing dealt with determining pressure amplitudes as a function of gage location, blade number, propeller diameter, propeller advance, and Reynolds number. Pohl also conducted pressure measurements on hull surfaces near the propellers on ship models. He made some comparisons between the experimental results he obtained and the predictions of Breslin's theory and his own calculation method.[3]

In 1963, Kowalski and Breslin[4] reported pressure measurement results obtained in the towing basin at Davidson Laboratory. Their measurements were taken in free space, on a flat plate, and on circular cylinders of different diameters. In these experiments, the pressure measuring devices remained stationary and the rotating propeller moved by at a constant velocity.

At present, considerable information exists on the nature of field pressure amplitudes, but only Pohl did any serious work in the determination of pressure phases. This knowledge is of crucial importance in determining hull vibration.

The present experiments were initiated mainly to evaluate the reliability of the predictions of pressure amplitude and phase of the new calculation method of Kerwin and also to investigate the effect on induced pressures of various parameters of propeller geometry and flow conditions not heretofore considered. The significant contribution of this work was a technique to separate experimentally the loading and thickness portions of the total signal. Also included were limited comparisons between experimental results and the predictions of Breslin's method. Both theories, Kerwin's and Breslin's, offer separate procedures for determining the effects of blade thickness on field-point pressures; the two solutions are, however, formulated differently.

Kerwin's method is an extension of his lifting-surface propeller design theory[5] and is applicable to moderately loaded propellers. It is based on a vortex lattice representation of blade loading and utilizes a linearized source-sink distribution to represent blade thickness. A point-wise distribution of the axial, radial, and tangential velocities is calculated relative to a propeller blade, a harmonic analysis of this distribution is performed, and the linearized, blade-rate pressure coefficient is derived from the induced velocities. Although the method incorporates quite an intricate numerical evaluation, it has been programmed for the IBM 7090 and the input procedure is straightforward.

Breslin's method, not available in computer program form at the time of these calculations,* but adaptable to straightforward hand calculation, is based on a lifting-line representation of the propeller blade. The procedure assumes the propeller to be lightly loaded and an independent thickness effect calculation is obtained by assuming a sector blade outline form. The blade-rate pressure coefficient, $K_p = \frac{\Delta p}{\rho N^2 D^2}$, is consistent in both methods.

Presented first in this report will be the results of pressure measurements carried out in uniform flow and the comparisons of these with the blade-rate pressure coefficients obtained from theoretical calculations. The last portion of the report presents experimental pressure results from investigations of such parameters as propeller geometry, propeller blade cavitation, and nonuniform inflow, but no comparisons with theory have been made.

TEST PROCEDURE

EXPERIMENTAL TECHNIQUE

All experimental results presented in this discussion are from measurements obtained on a flat plate located parallel to the propeller axis in the 24-inch water tunnel. A sketch of the tunnel setup is shown in Figure 1 along with the flat plate dimensions and pressure transducer locations. The plate was positioned such that the two transverse gages were at the plane of the propeller, i.e., the plane formed by the blade centerlines. Some axial variations in the plate location relative to the propeller plane occurred during the different tests due to slight differences in propeller hub lengths and the space limitation when the wake screen was in place; these small axial shifts are shown in the presentation of experimental data points.

A detailed schematic of the apparatus circuitry is presented in the appendix with further description of the components involved. Tests were run in a 27-inch-diameter closed-jet section with the propeller(s) fitted on the downstream shaft. Water speeds were determined by setting a thrust identity with the open-water test results. The use of the variable-pressure water tunnel facility made it possible to determine the effect on induced field pressures of propeller cavitation. The closed-jet test section enabled the use of wake screens (designed by the method of Reference 6) for the generation of nonuniform flows and for the determination of the effect of those flows on induced pressures.

The majority of the experimental work was performed with two model propellers, numbered 4118 and 4119. A drawing of Propeller 4118 is shown in Figure 2 along with some pertinent design information. Propeller 4119 had twice the thickness of 4118 and a slight

*During the Workshop on Fluctuating Propeller Forces Held at DTMB on 21 and 22 April 1966, Dr. Chengi Kuo presented pressure calculations obtained from his programmed version of Breslin's method. In his numerical evaluation, Kuo was able to eliminate certain hampering assumptions necessary in Breslin's analytic solution.

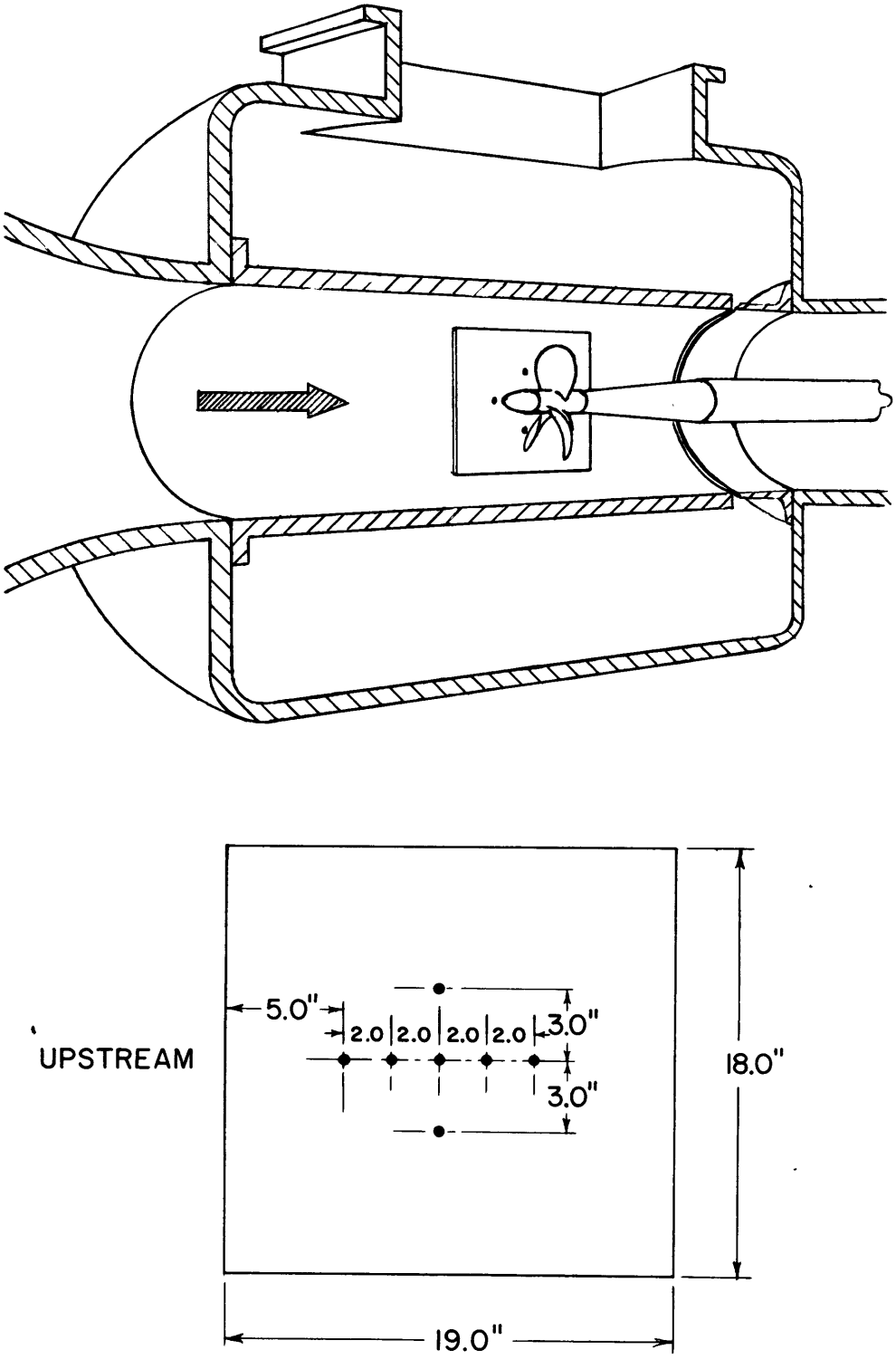

Figure 1 – Flat Plate Dimensions and Placement in the Water Tunnel

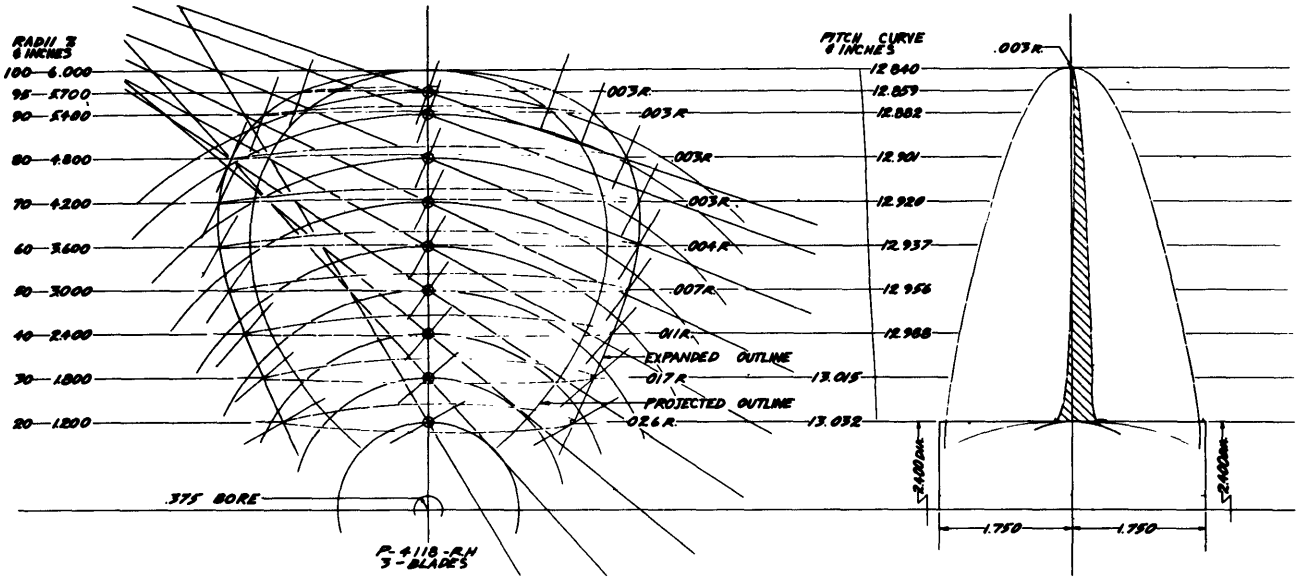

r/R	ℓ/D	f/ℓ	P/D	t/ℓ	$G_{0.833}$	$G_{1.16}$	$G_{0.6}$
0.2	0.3200	0.0142	1.0860	0.1028	0.0	0.0	0.0
0.3	0.3635	0.0232	1.0845	0.0776	0.0209	0.0002	0.0479
0.4	0.4048	0.0230	1.0823	0.0590	0.0287	0.0002	0.0646
0.5	0.4392	0.0218	1.0796	0.0451	0.0334	0.0003	0.0753
0.6	0.4610	0.0207	1.0780	0.0348	0.0356	0.0003	0.0806
0.7	0.4622	0.0200	1.0766	0.0271	0.0355	0.0003	0.0807
0.8	0.4347	0.0197	1.0750	0.0210	0.0327	0.0003	0.0750
0.9	0.3613	0.0182	1.0735	0.0166	0.0256	0.0002	0.0593
1.0	———	———	1.0700	———	0.0	0.0	0.0

Figure 2 – Propeller 4118 Drawing and Design Information with the Bound Circulation Distributions at Off-Design Conditions

pitch correction due to the added thickness, the development of which is inherent in the design method. Open-water test results for both propellers are shown in Figures 3 and 4.

The propellers were designed using Lerb's induction factors[7] and the lifting-surface corrections of Kerwin.[5] Both propellers were 12 inches in diameter and had an expanded area ratio of 0.60 and TMB modified thickness sections with $a = 0.8$ mean lines. The propellers were run at three advance conditions, $J = 0.60$, $J = 0.833$ (design J), and $J = 1.160$ (the zero thrust condition). Shaft revolutions were set at 12.0, 18.0, and 25.0 rps for the three advance conditions, and Reynold's number values at the 0.7 radius ranged from 1.5×10^6 to 3.0×10^6. Pressures on the flat plate were measured during the three advance conditions for propeller tip clearances of 10 and 30 percent of the propeller radius.

The test procedure involved several minutes of pressure recording at a particular propeller operating condition. These pressures were recorded simultaneously from the seven transducers onto magnetic tapes. An on-line record was kept of wave analyzer results of each pressure signal and was used later to check the tape data. The transducers were statically calibrated after every third test and all transducers retained a linear response throughout the experiments. Two typical calibration curves are shown in Figure 5.

Taped pressure records consisted of a recorded signal for each 3 degrees of propeller rotation. These were triggered by a 120-tooth gear attached to the propeller shaft. A single-toothed gear was also attached to the shaft. The lone tooth, alined with one of the blades, triggered a single magnetic pulse per propeller revolution when the blade centerline was normal to the plate. The single pulse, recorded simultaneously with the pressure signals, was used for data phase analysis. From the lengthy records, data from no less than 100 propeller revolutions were digitized and averaged. Figure 6 shows a typical average wave form.

A harmonic analysis of the average pressure wave was performed, and from the harmonic analysis it was obvious that, except for the shaft rate harmonic, the only harmonics of any consequence were those of blade rate and multiples of blade rate. Although not very discernible in Figure 6, the amplitude of the shaft harmonic was on occasion as much as 50 percent of that of blade rate and it was particularly distinguishable in data taken during lightly loaded conditions or at far points up and downstream of the propeller. Recent examinations suggest that the high shaft rate signal can be attributed to shaft misalinement and/or constructional irregularities in the propellers.

Of the harmonics higher than blade rate, the amplitude of twice the blade-rate harmonic was by far the largest. Figure 7 shows the phase and amplitude of the blade-rate and twice blade-rate harmonics for design operating condition.

ANALYSIS

A simple treatment of the experimental data was necessary for its comparison with the theoretically calculated values. The unsteady pressure at each transducer can be represented by a Fourier series:

(Text continued on page 12.)

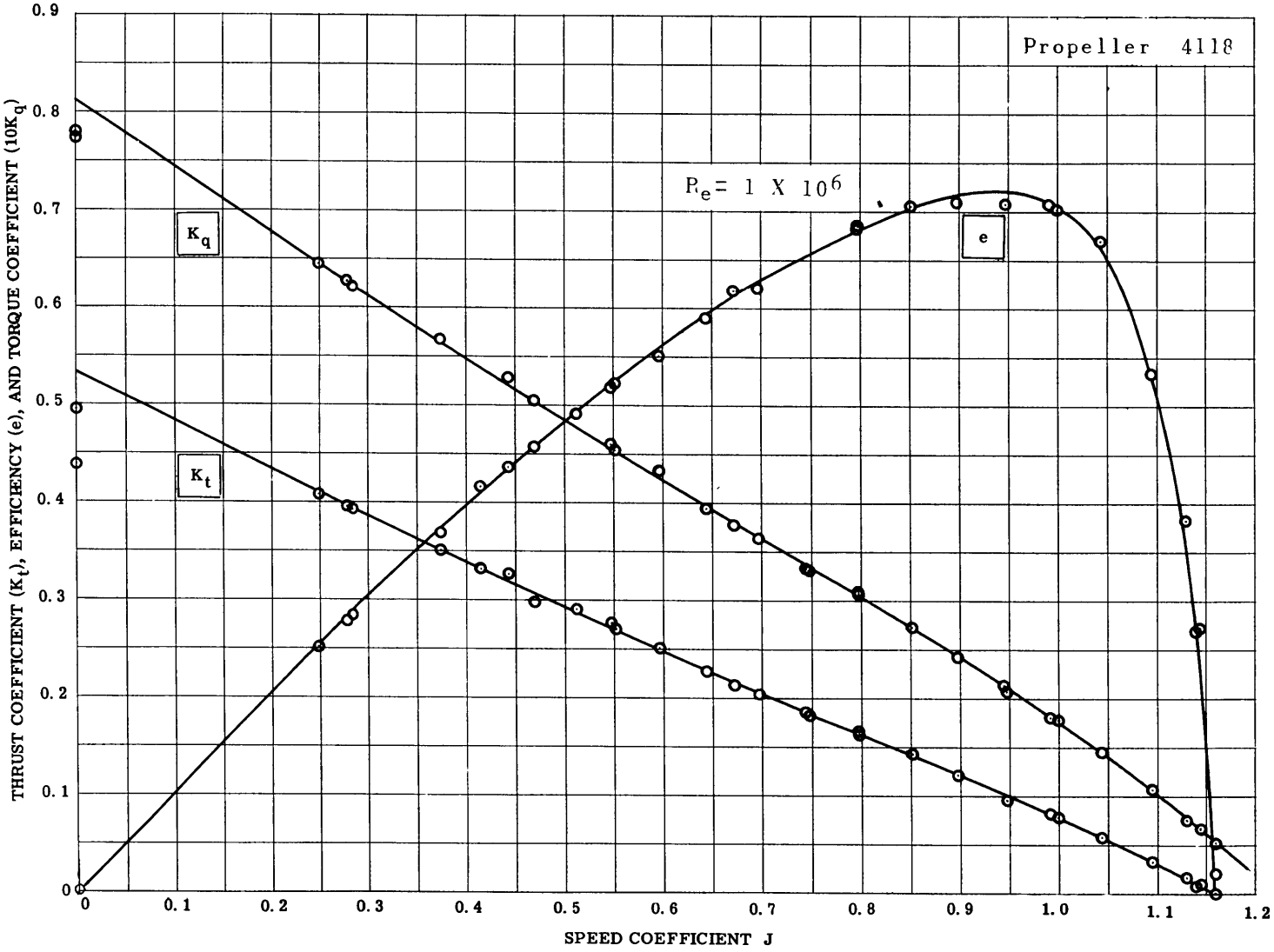

Figure 3 – Open-Water Performance Curves, Propeller 4118

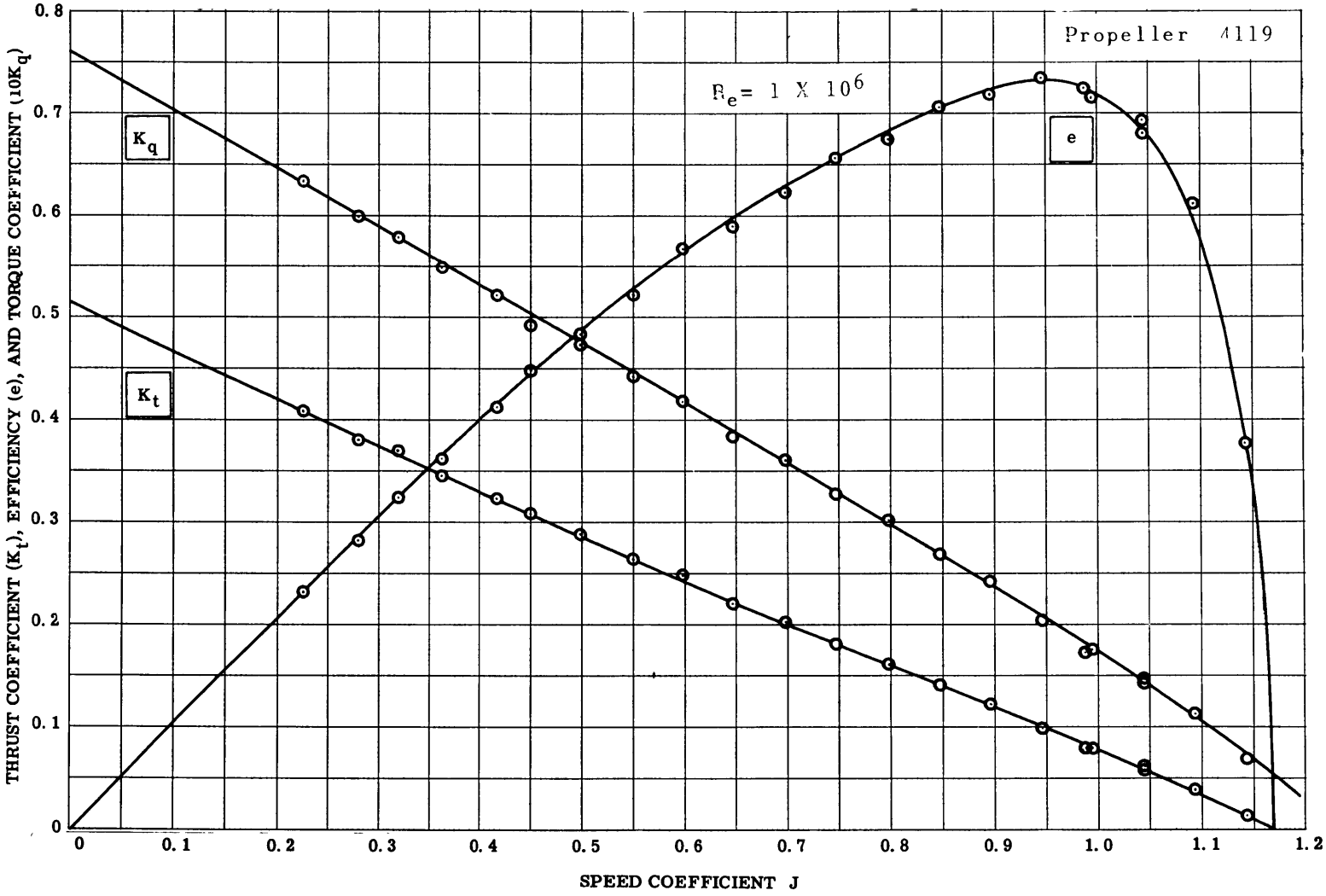

Figure 4 – Open-Water Performance Curves, Propeller 4119

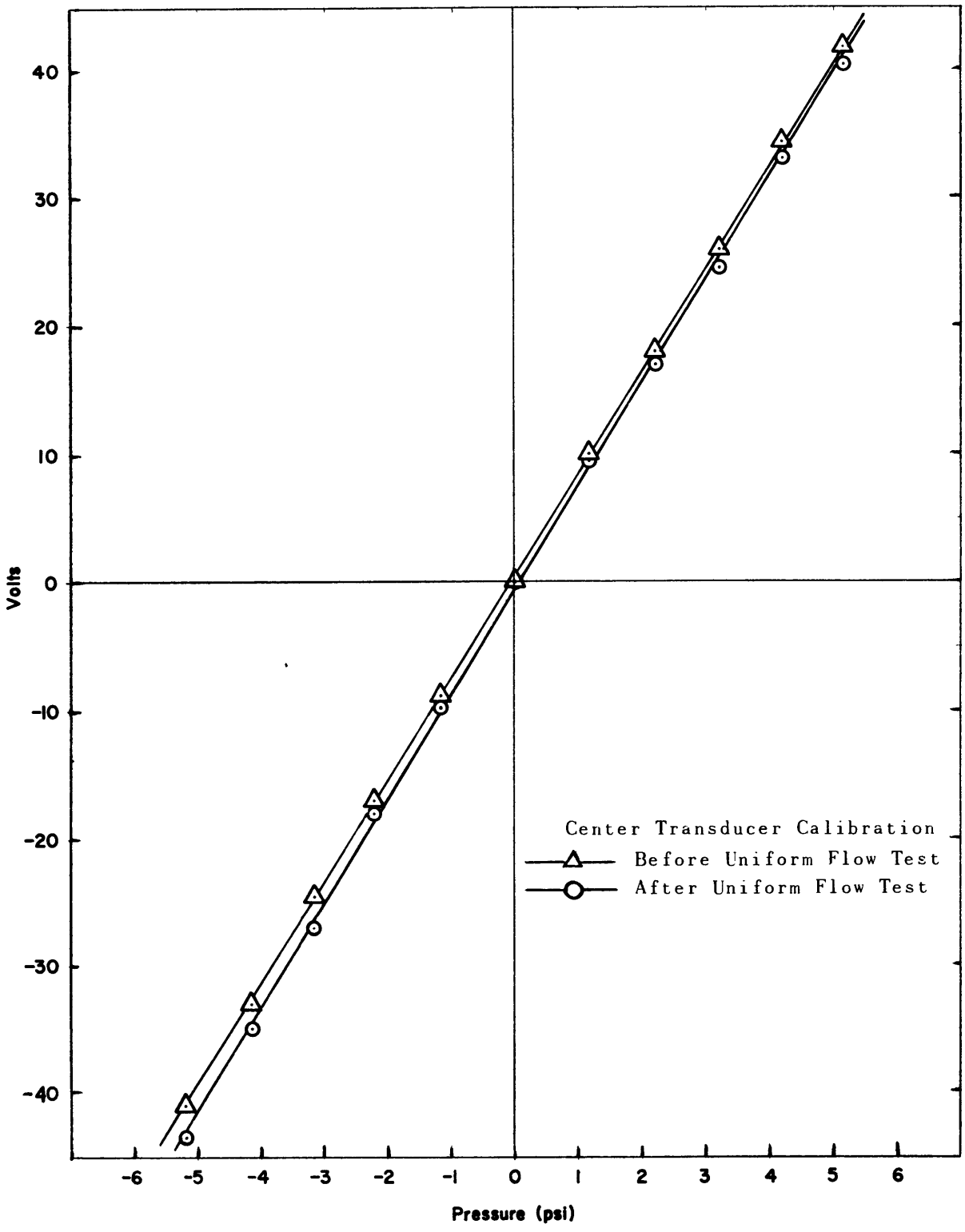

Figure 5 – Sample Successive Calibration Curves for One Pressure Transducer

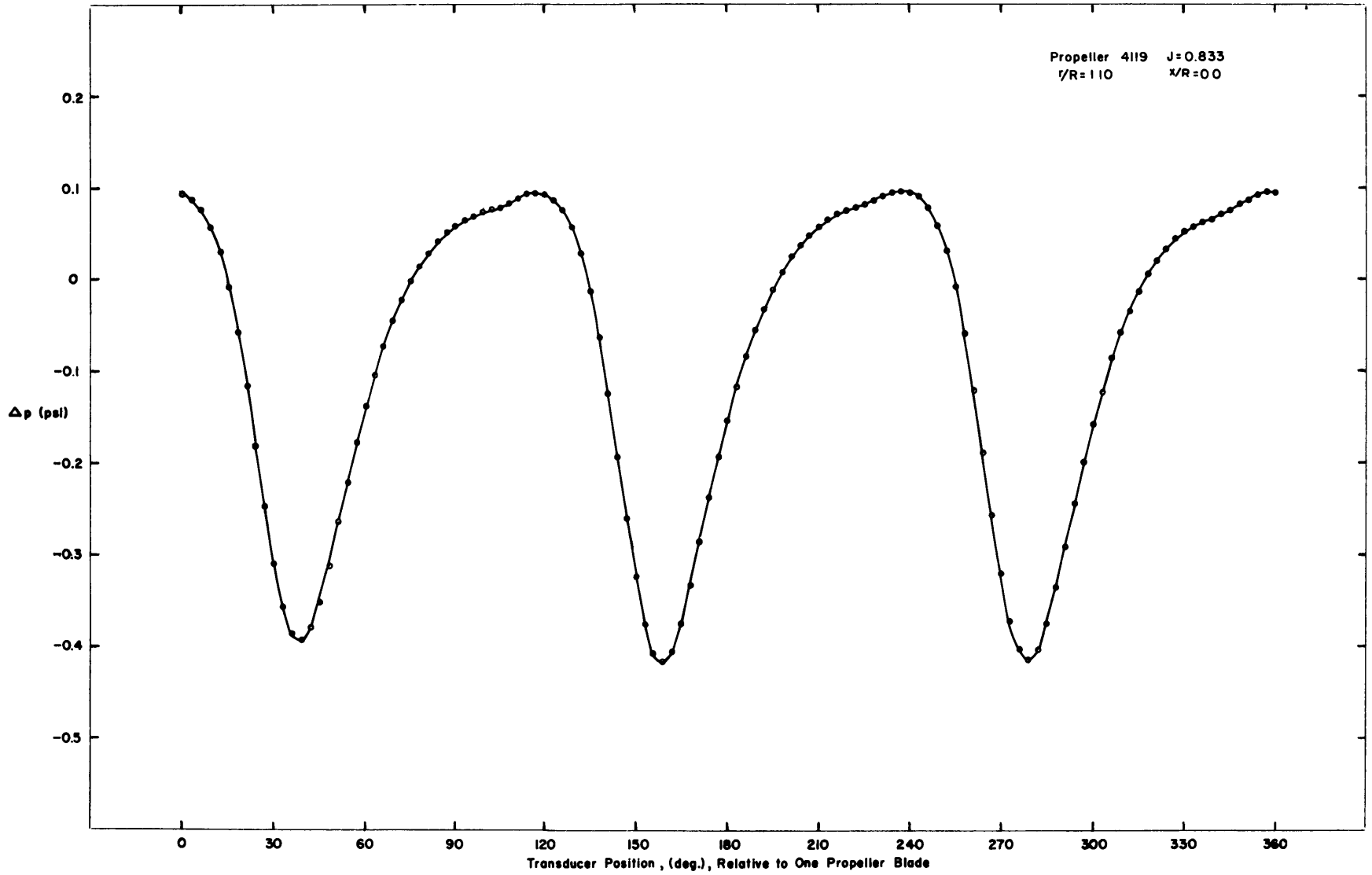

Figure 6 – Typical Average Pressure Wave (100 Samples)

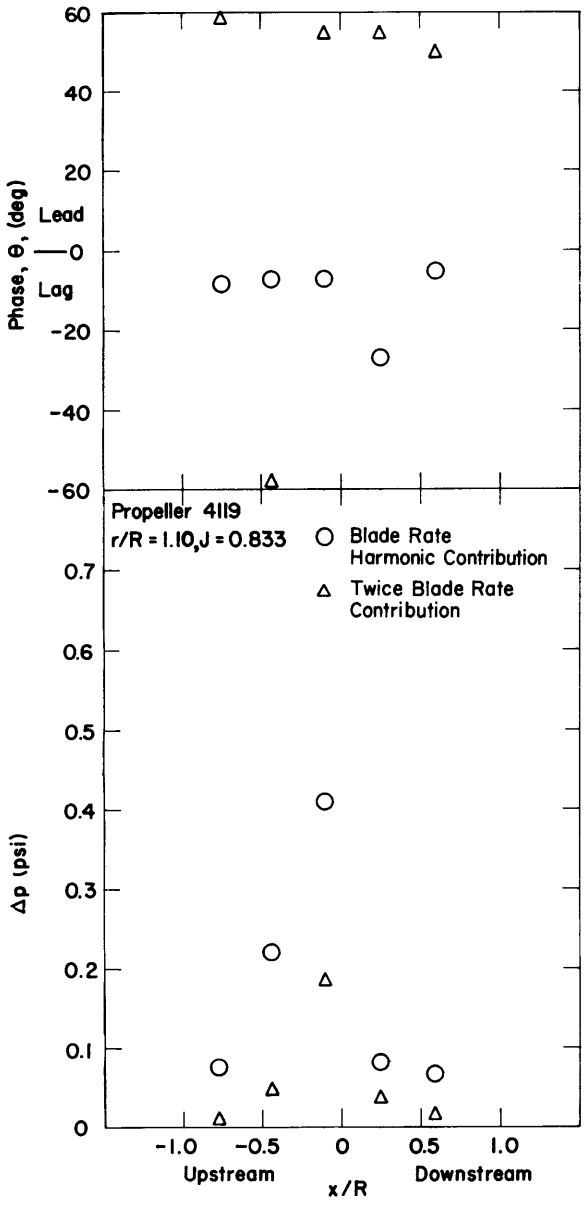

Figure 7 – Phase and Amplitude of the Blade-Rate and Twice Blade-Rate Harmonics for One Operating Condition

$$p = \frac{a_0}{2} + \sum_{m=1}^{\infty} a_m \cos m\phi + b_m \sin m\phi \qquad [1]$$

and the blade-rate pressure amplitude would be:

$$\Delta p = c_n = [(a_n)^2 + (b_n)^2]^{1/2} \qquad [2]$$

where n is the number of blades.

The phase of the blade-rate signal was derived from:

$$p = \frac{a_0}{2} + \sum_{m=1}^{\infty} c_m \left(\frac{a_m}{c_m} \cos m\phi + \frac{b_m}{c_m} \sin m\phi \right)$$

by letting

$$\frac{a_m}{c_m} = \cos \gamma \quad \text{and} \quad \frac{b_m}{c_m} = \sin \gamma$$

Therefore

$$p = \frac{a_0}{2} + \sum_{m=1}^{\infty} c_m \cos(m\phi - \gamma)$$

and by neglecting all terms except those of blade rate

$$\tan \gamma = \frac{b_n}{a_n} \quad \text{or} \quad \gamma = \tan^{-1} \left(\frac{b_n}{a_n} \right)$$

The maximum blade-rate signal occurs when $(n\phi - \gamma) = 0$. Therefore when $\phi = \frac{\gamma}{n}$ the phase angle θ for which $(\Delta p)n$ is a maximum is defined to be

$$\theta = \frac{1}{n} \tan^{-1} \frac{b_n}{a_n} \qquad [3]$$

The experimental pressure amplitudes were then nondimensionalized as follows:

$$K_{p_n} = \frac{\Delta p}{\rho N^2 D^2}$$

Separation of the thickness and loading portions of the total blade-rate signal at each transducer came about simply in the analysis of the pressure data for both propellers, 4118 and 4119. If we assume that the thickness contribution to the field pressure is linear, the blade-rate coefficients of the thickness contribution can be determined by subtracting, in phase, the blade-rate coefficients of the total signal induced by Propeller 4118 from those induced by the double-thickness propeller, 4119, at identical operating conditions. The blade-rate coefficients of the loading signal can, in turn, be obtained by subtracting the thickness contribution coefficients from the total blade-rate signal of parent Propeller 4118. The amplitudes and phases of thickness and loading follow directly by Equations [2] and [3].

Since the theories predict free-space blade-rate pressures, all calculated values were doubled for comparison with the results of the flat-plate measurements in accordance with the assumptions of an infinite flat plate and a consequent pure image effect. This procedure is valid in the limited cases in which the calculated free-space induced axial and tangential (relative to the propeller) velocity vectors are parallel to the plate and the radial component is normal to it.

RESULTS

COMPARISON OF EXPERIMENTAL RESULTS WITH THEORY

Design *J*

In addition to a separate thickness contribution, results from Kerwin's programmed method include the induced field point pressures due to the bound vortices, the lifting-line trailer vortices, and the correction for the trailers on the blade. These factors were added, in phase, to furnish the total loading contribution presented in the comparisons which follow. Figure 8 shows the amplitudes and phases of each of the loading factors and the resulting summation for a representative case at design operating condition.

Figures 9, 10, and 11 show the total blade-rate signal, the thickness contributions, and the loading contributions, respectively, for Propeller 4118 operating at design advance coefficient, $J = 0.833$, and at a tip clearance of 10 percent of the radius. Theoretical predictions obtained by both Kerwin's and Breslin's methods are superposed onto the plots of the experimental values. Since the experimental results from the two transverse gages on the plate in the plane of the propeller, in Figure 1, are not applicable to direct theoretical comparison, only the data from the five axial transducers will be presented.

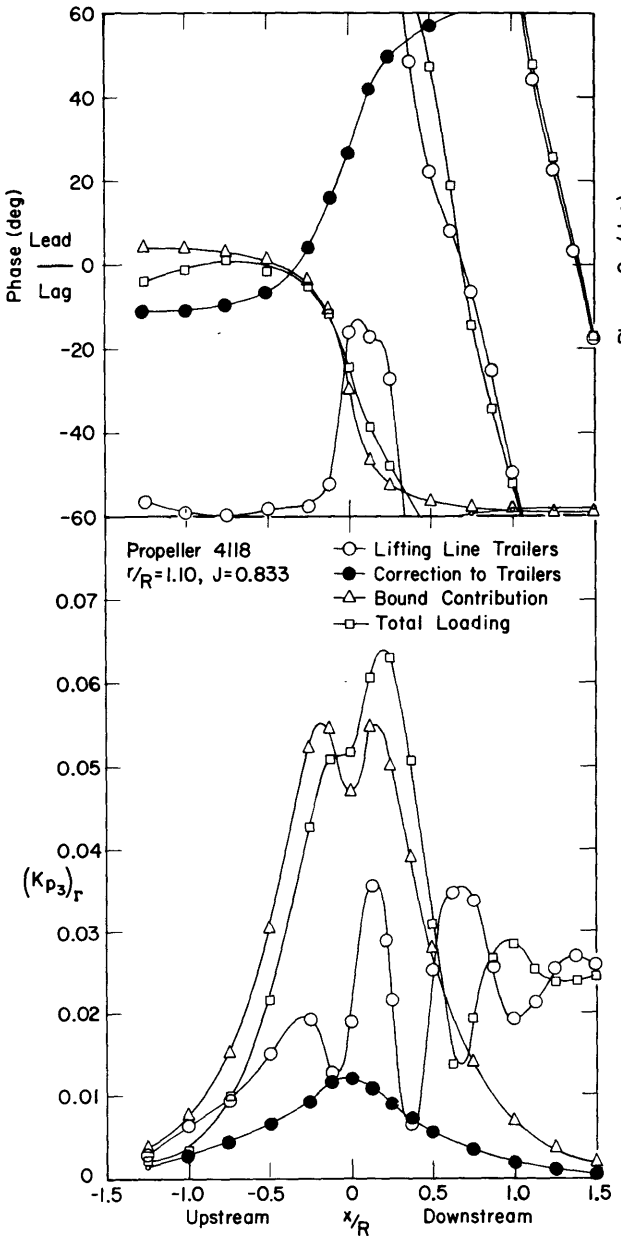

Figure 8 – Individual Loading Contributions and Phase Defined in Kerwin's Method

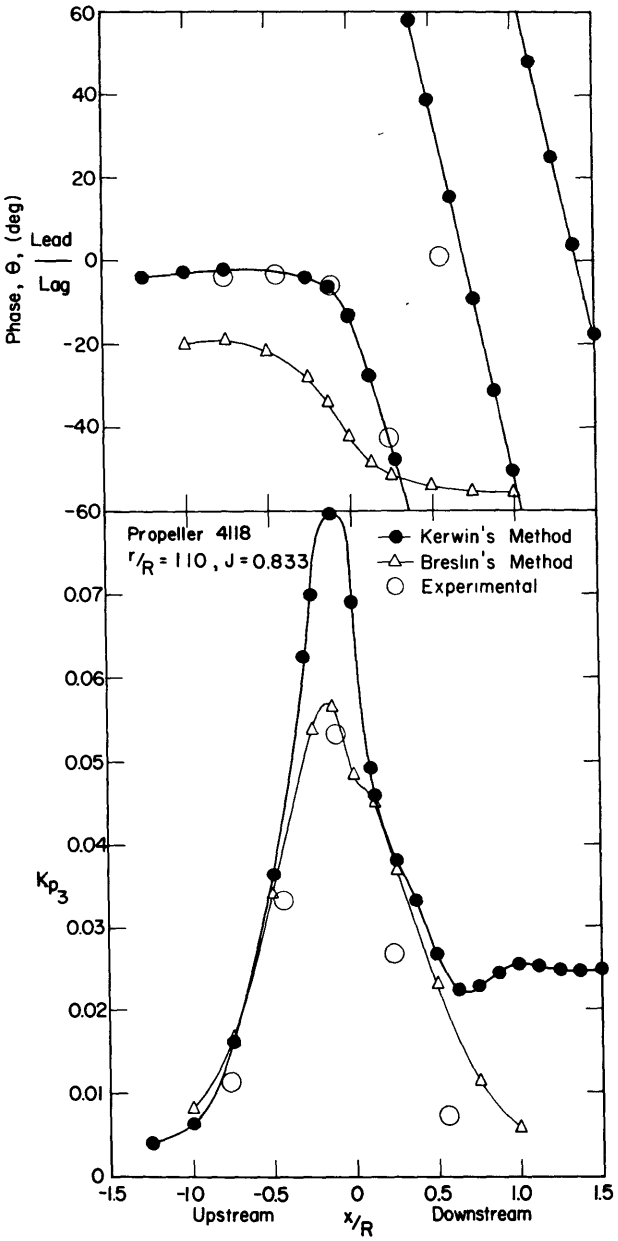

Figure 9 – Comparisons of Theoretical and Experimental Values, Total Blade-Rate Signal, r/R = 1.10, J = 0.833

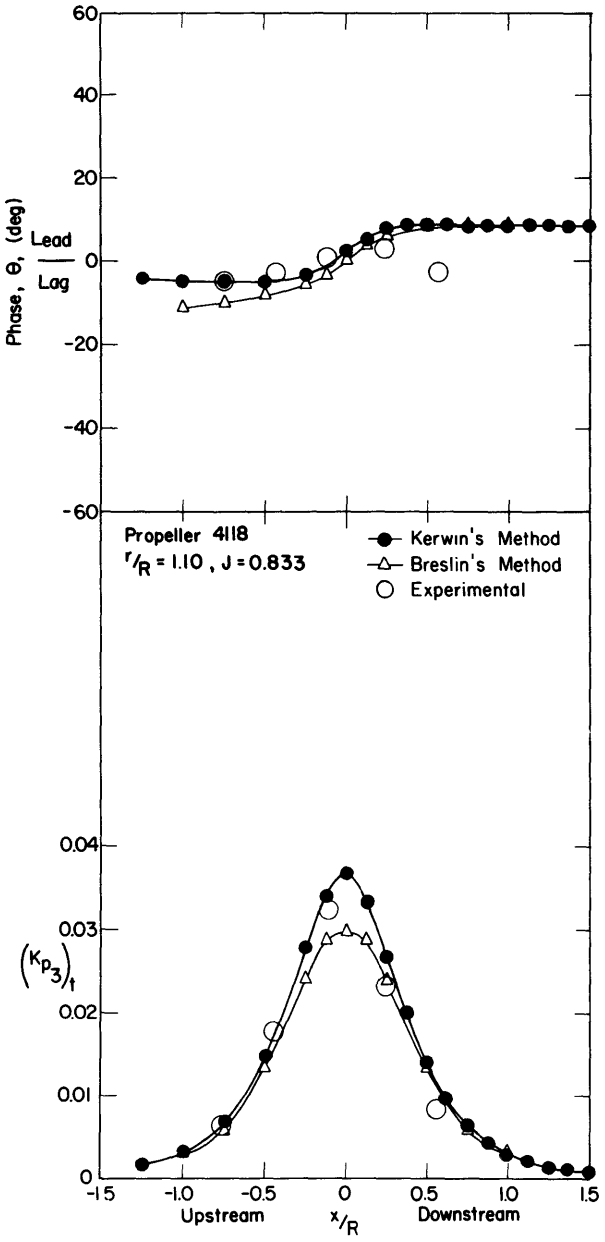

Figure 10 – Comparisons of Theoretical and Experimental Values, Thickness Contribution, r/R = 1.10, J = 0.833

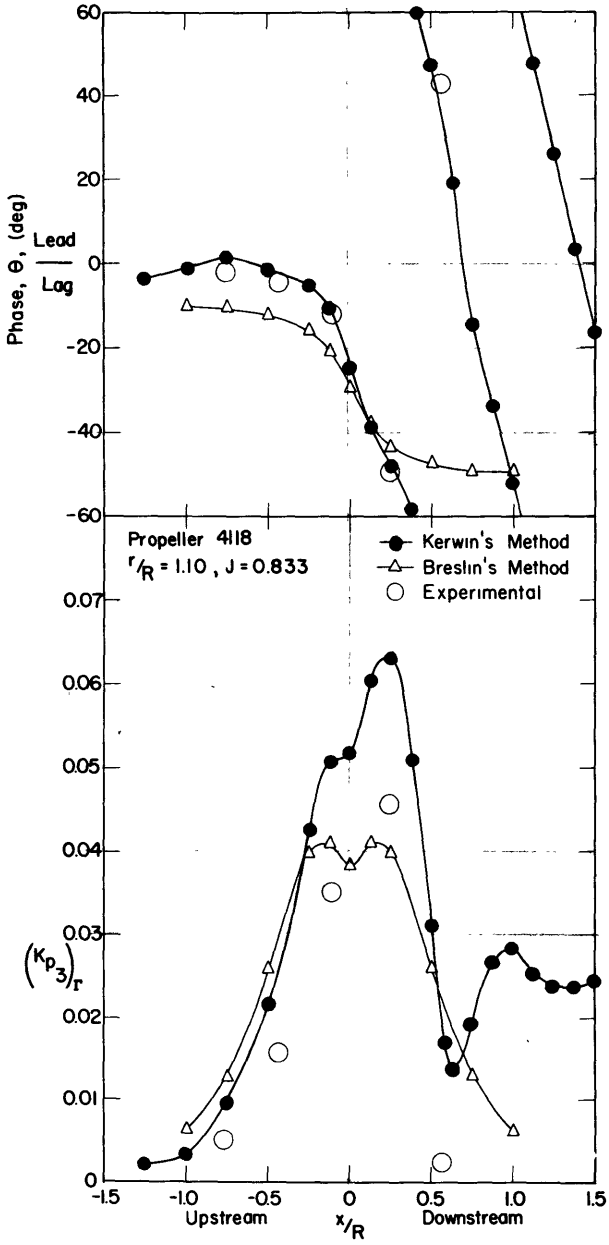

Figure 11 – Comparisons of Theoretical and Experimental Values, Loading Contribution, r/R = 1.10, J = 0.833

It is obvious in Figure 10 that both theories predict equally well the amplitudes and phases of the blade-rate thickness contributions. However, in the plots of the loading contribution, sizable discrepancies can be noted between the predictions of the two methods and the experimental results. Upstream of the propeller, the calculated amplitudes lie within the expected accuracy, but downstream of the propeller plane both methods tend to predict higher pressures than were experimentally found to exist. The downstream pressures calculated by Kerwin's method failed to diminish and, instead, leveled off. The predictions of blade-rate phases of Kerwin's method were very good with the exception of a shift in the downstream values of the total signal phase, and this was due primarily to the similar shift in the calculated thickness contribution phases. Phases calculated with Breslin's method were poor for the entire axial comparisons of the loading signals.

These plots concluded the calculations with Breslin's method. Subsequent comparisons were made between experimental results and predictions of Kerwin's theory alone and were extended to checking his method's reliability in predicting pressures at off-design operating conditions.

Figures 12, 13, and 14 show the comparisons between experimental results and the predictions of Kerwin's method for a tip clearance of 30 percent of the radius and for the propeller still operating at design advance. Prediction of the thickness contribution amplitude is still good but the thickness phase prediction downstream disagrees with experiment as it did at the smaller propeller tip clearance. Prediction of the total blade-rate amplitude and phase is improved at the greater clearance, but the calculated loading amplitude is in poor agreement with experiment, particularly upstream.

In the preceding plots it was noted that the calculated blade-rate pressures due to loading fail to diminish downstream. This characteristic is even more noticeable in later comparisons in which the propeller was heavily loaded and had stronger resulting trailing vortices. At first it was suspected that this phenomenon was the fault of an incorrect numerical evaluation of these trailers inherent in the Kerwin method. Therm Advanced Research, Inc.[8] was asked to make a check, and calculations of the resulting downstream velocities were performed for the same propeller and operating conditions. The calculation method at Therm is similar to Kerwin's but was developed independently. Therm's calculated downstream velocities were in near-exact agreement with Kerwin's.

The next step was to investigate the possible effects of slipstream contraction and axial elongation of the trailing vortices. Calculations showed that at a distance of one radius downstream the slipstream contraction should be less than 3 percent of the propeller diameter for Propeller 4118 operating at its design advance. Consequently, the pressures on the flat plate should not be appreciably affected by the slight increase in distance from the downstream trailers. To check the axial elongation of the trailers, Kerwin's program was input

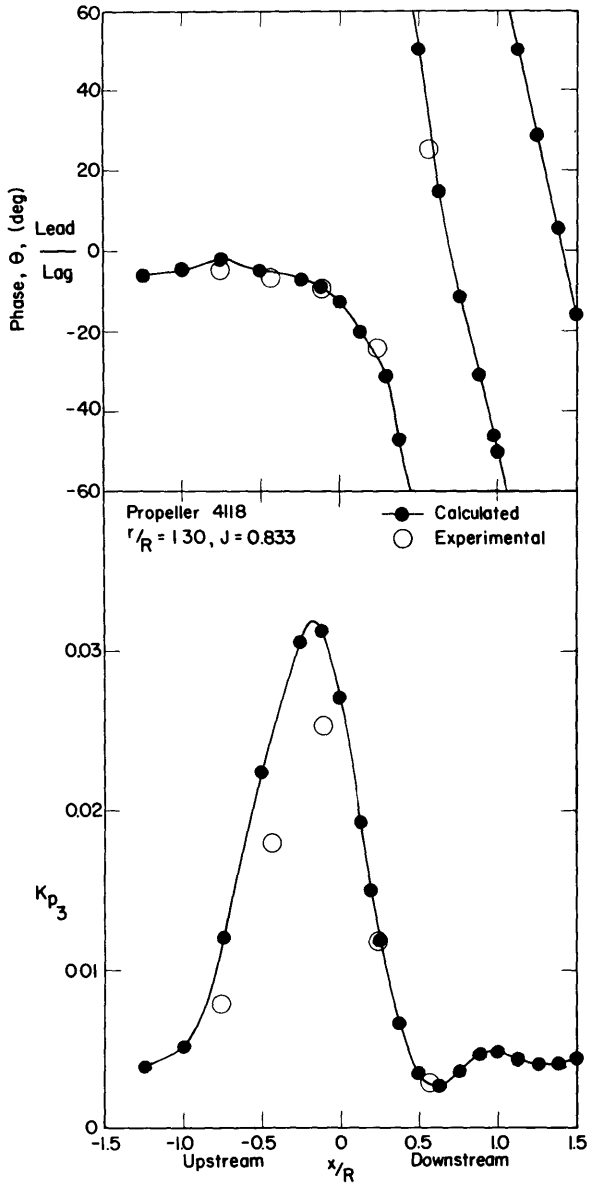

Figure 12 – Comparison of the Predictions of Kerwin's Method and Experimental Values, Total Blade-Rate Signal, r/R = 1.30, Design J

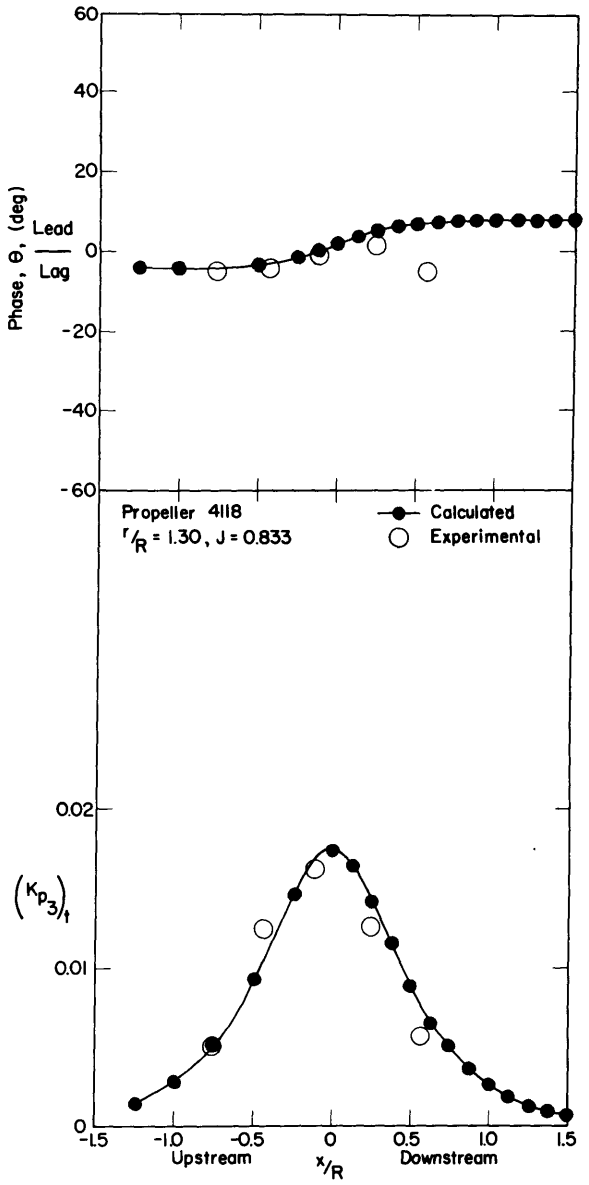

Figure 13 – Comparison of the Predictions of Kerwin's Method and Experimental Values, Thickness Contribution, r/R = 1.30, Design J

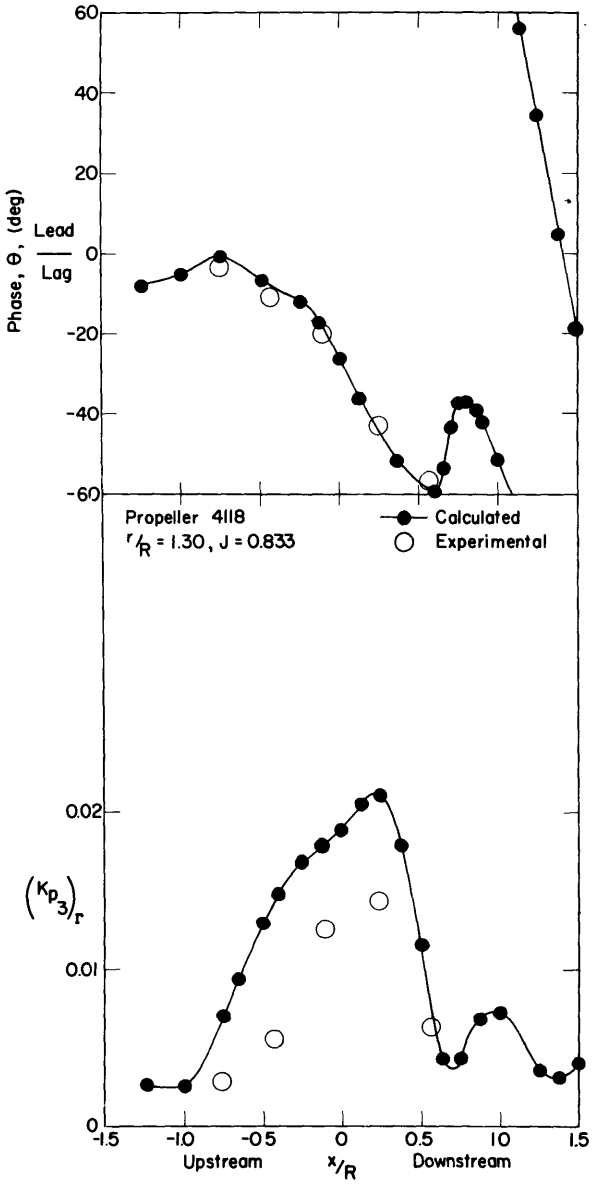

Figure 14 – Comparison of the Predictions of Kerwin's Method and Experimental Values, Loading Contribution, r/R = 1.30, Design J

with an increased pitch at the lifting line equal to the ultimate pitch angle. Figure 15 shows that this procedure did not reduce the calculated amplitudes but, to the contrary, increased the predicted amplitudes downstream.

Calculations were also performed, by hand, to determine whether or not the linearization of the pressure equation made any appreciable differences in the results using Kerwin's method. As expected, it did not; the linearized results were slightly lower. Results of both calculations are shown in Figure 16 for the 10-percent radial tip clearance with Propeller 4118 operating at design advance.

Downstream pressure predictions from Kerwin's theory are questionable if only in the failure of the calculated signal to diminish far aft of the propeller. The experiments done here and those of Pohl[2] and Breslin[4] show a rapid decay in the pressure signals as the downstream distance from the propeller is increased. That the experimental results are in error is also possible, but as Pohl pointed out in his work, any flow distortion caused by the presence of the plate or boundary layer buildup on the plate would cause a heavier loading of the propeller blade and result in greater induced field pressures. Therefore, it is probable that the experimentally determined pressures presented in this work are not significantly reduced in magnitude by any oversight in the experimental procedure or analysis.

Heavily Loaded Advance Condition

Figures 17 through 22 show the comparison between the predictions using Kerwin's method and experimental results for the two tip clearances and for Propeller 4118 operating at a $J = 0.60$. Thickness and loading contributions are presented in addition to the total signal and were derived just as in the previous design advance coefficient cases. In the design J cases, however, input for the Kerwin program was directly obtainable from the propeller design data and the results of the Lerbs' induction factor calculations.[7] The necessary input data in part consists of the radial circulation distribution, the hydrodynamic pitch angle, the induced axial velocity distribution at the lifting line, and certain propeller geometry information. For the off-design advance ($J = 0.60$), the input data had to be obtained independently. An inverse propeller program for the quasi-steady calculation of alternating propeller thrust was altered to furnish the hydrodynamic conditions for Propeller 4118 operating at the off-design advance condition, $J = 0.60$.

For the heavily loaded cases (Figures 17 through 22) predictions using Kerwin's theory were good. In general, agreement between the calculated and experimental pressure amplitudes was comparable to that in the design advance coefficient case. Phase prediction was poorer, however, particularly downstream of the propeller.

Zero-Thrust Advance Condition

Figures 23 through 28 show the comparisons of the calculated pressures with those obtained while Propeller 4118 was operating at the zero thrust condition. Program input was

(Text continued on page 28.)

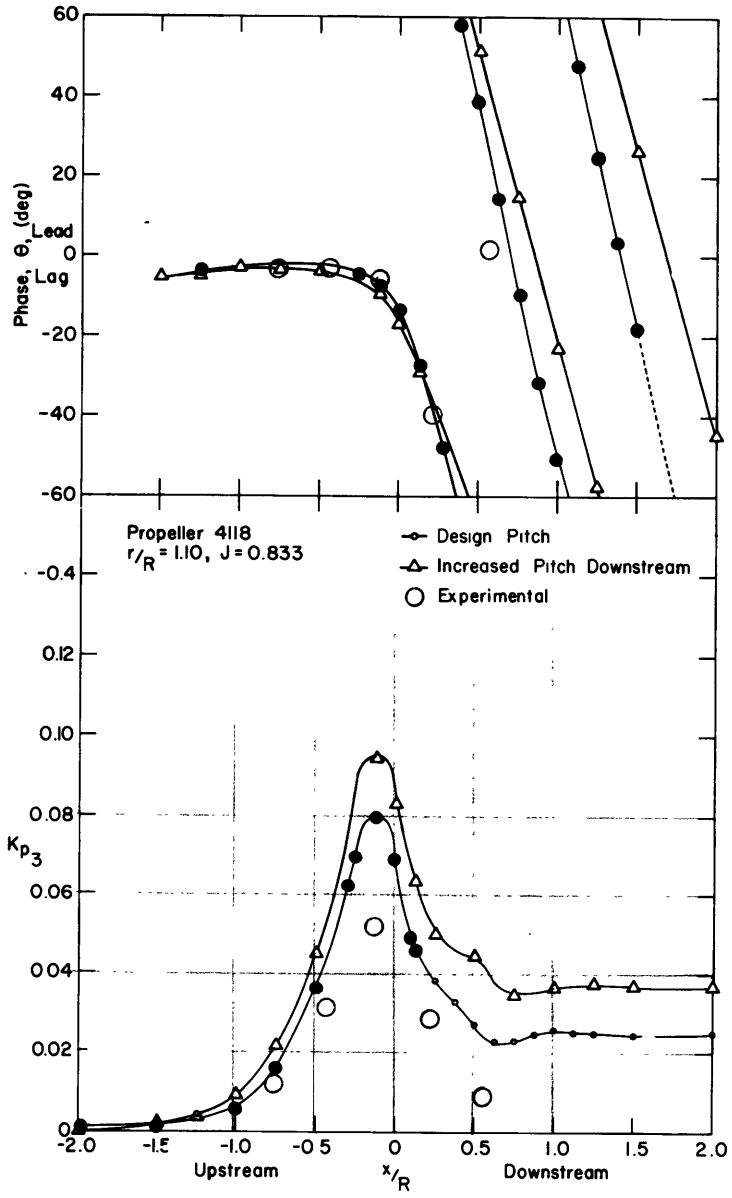

Figure 15 – Pressure Predictions of Kerwin's Method for Design Operating Condition and for an Imposed Increased Downstream Pitch

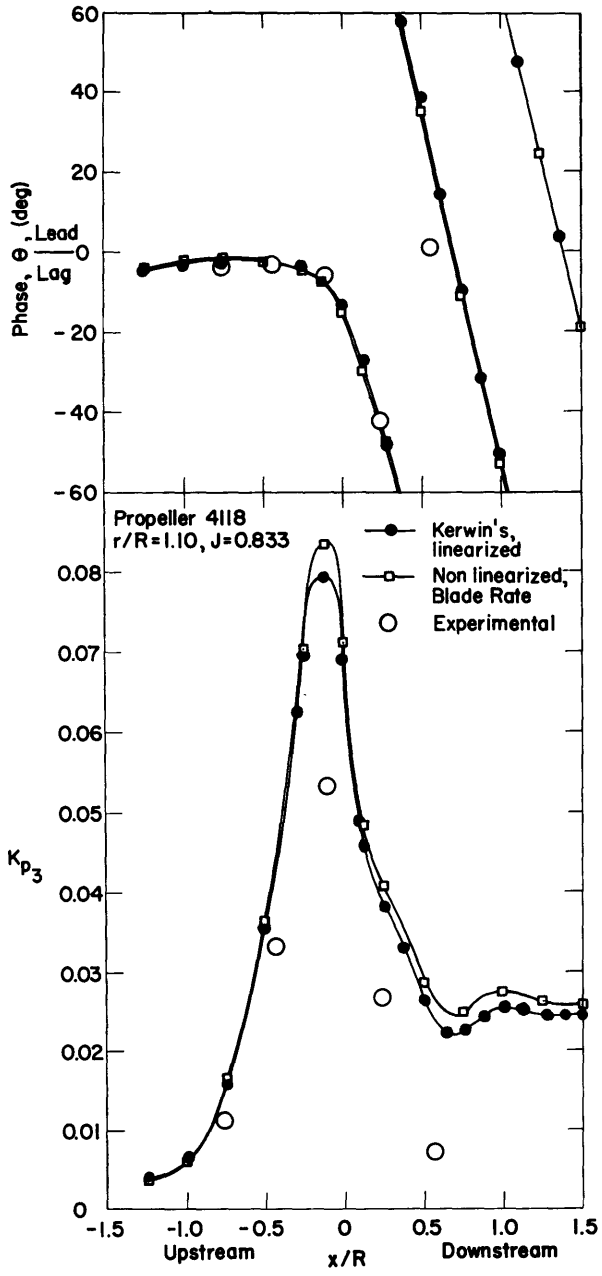

Figure 16 – Comparison of Linearized and Nonlinearized Total Blade-Rate Pressures

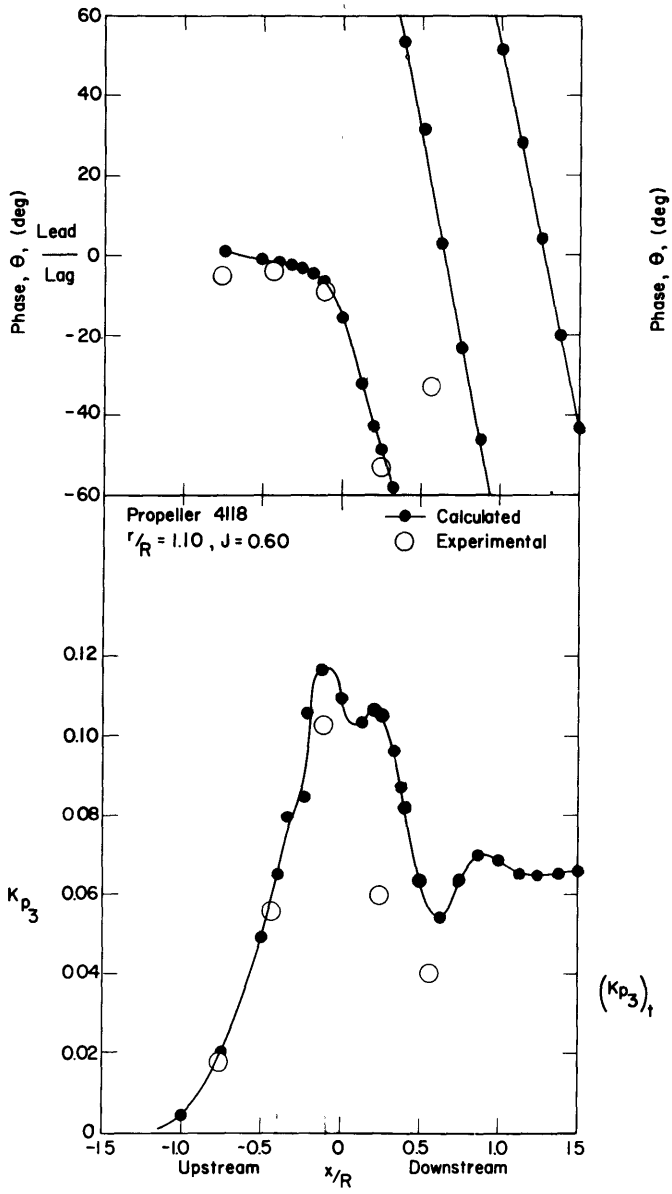

Figure 17 – Comparison of the Predictions of Kerwin's Method and Experimental Values, Total Blade-Rate Signal, r/R = 1.10, J = 0.60

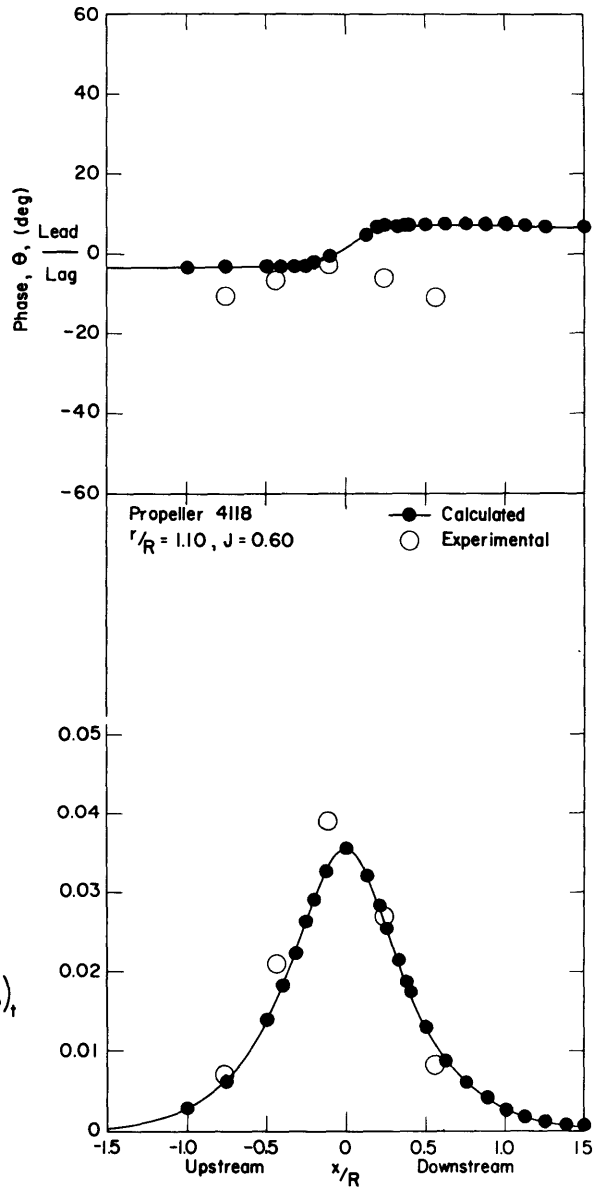

Figure 18 – Comparison of the Predictions of Kerwin's Method and Experimental Values, Thickness Contribution, r/R = 1.10, J = 0.60

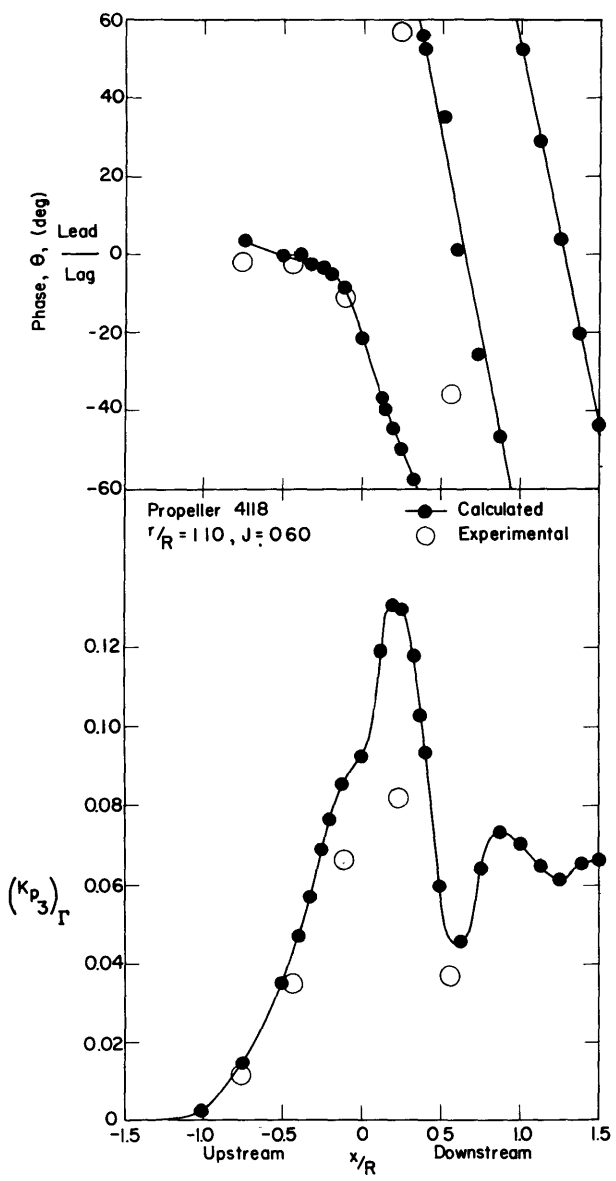

Figure 19 – Comparison of the Predictions of Kerwin's Method and Experimental Values, Loading Contribution, r/R = 1.10, J = 0.60

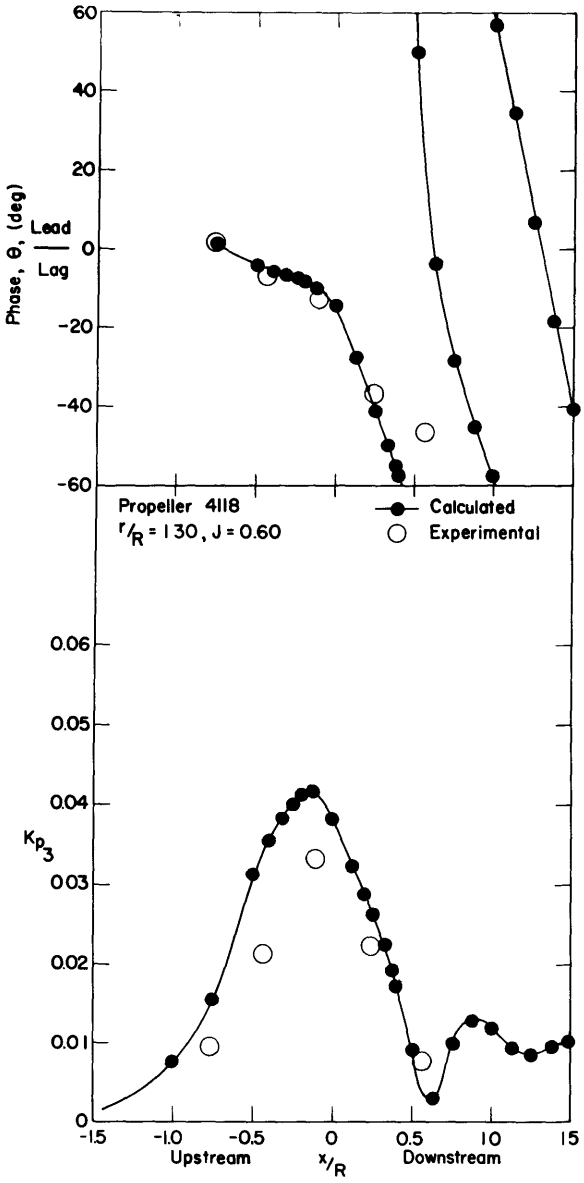

Figure 20 – Comparison of the Predictions of Kerwin's Method and Experimental Values, Total Blade-Rate Signal, r/R = 1.30, J = 0.60

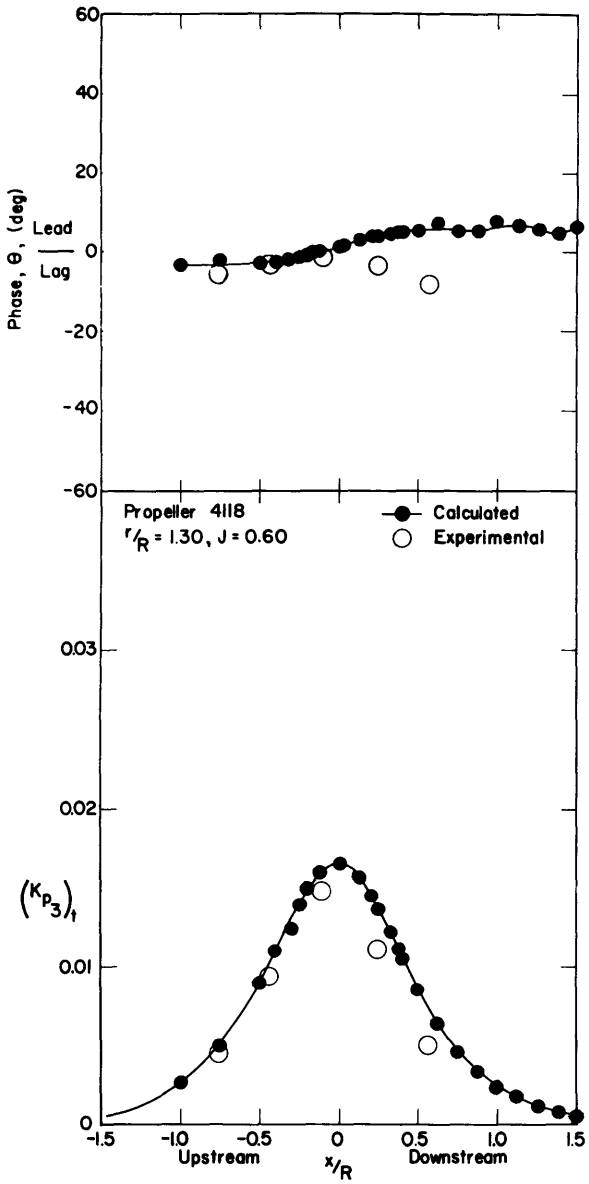

Figure 21 – Comparison of the Predictions of Kerwin's Method and Experimental Values, Thickness Contribution, r/R = 1.30, J = 0.60

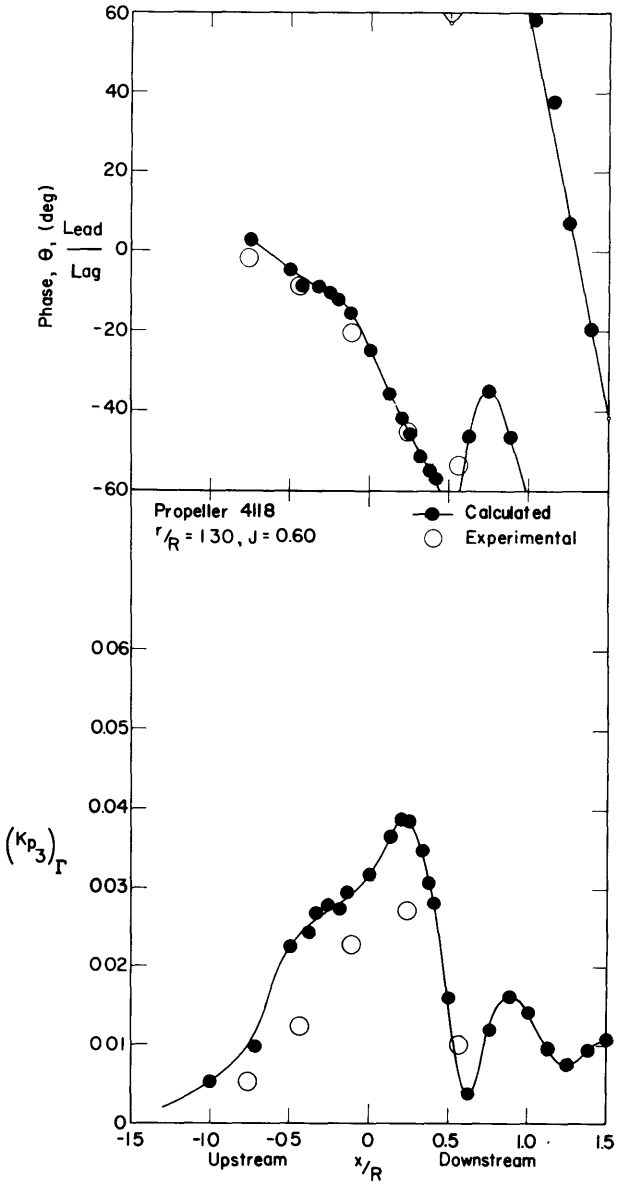

Figure 22 – Comparison of the Predictions of Kerwin's Method and Experimental Values, Loading Contribution, r/R = 1.30, J = 0.60

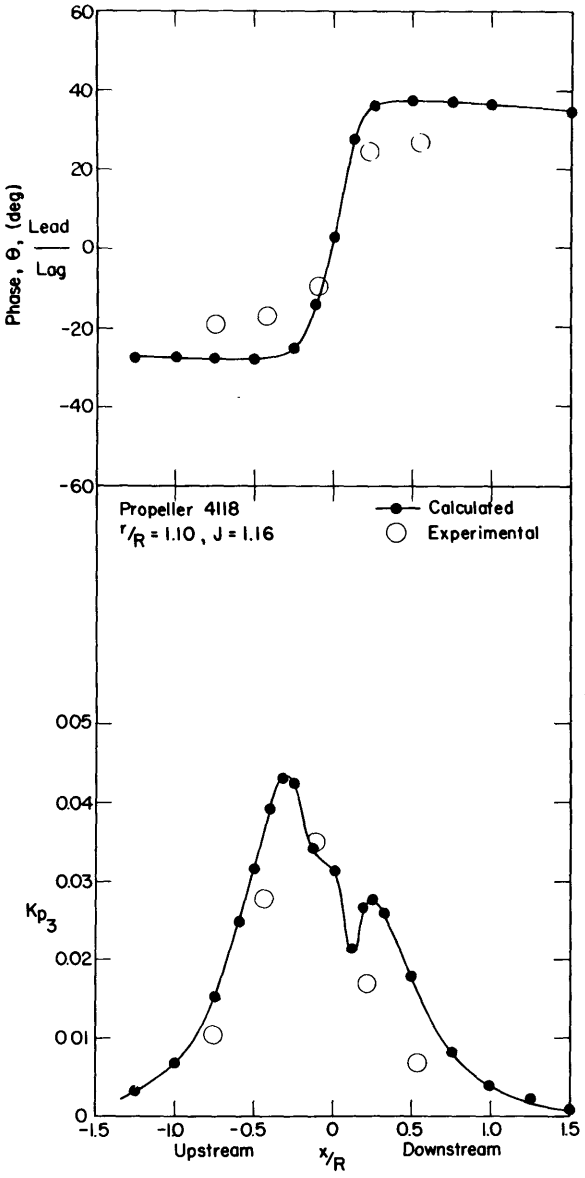

Figure 23 – Comparison of the Predictions of Kerwin's Method and Experimental Values, Total Blade-Rate Signal, r/R = 1.10, J = 1.16

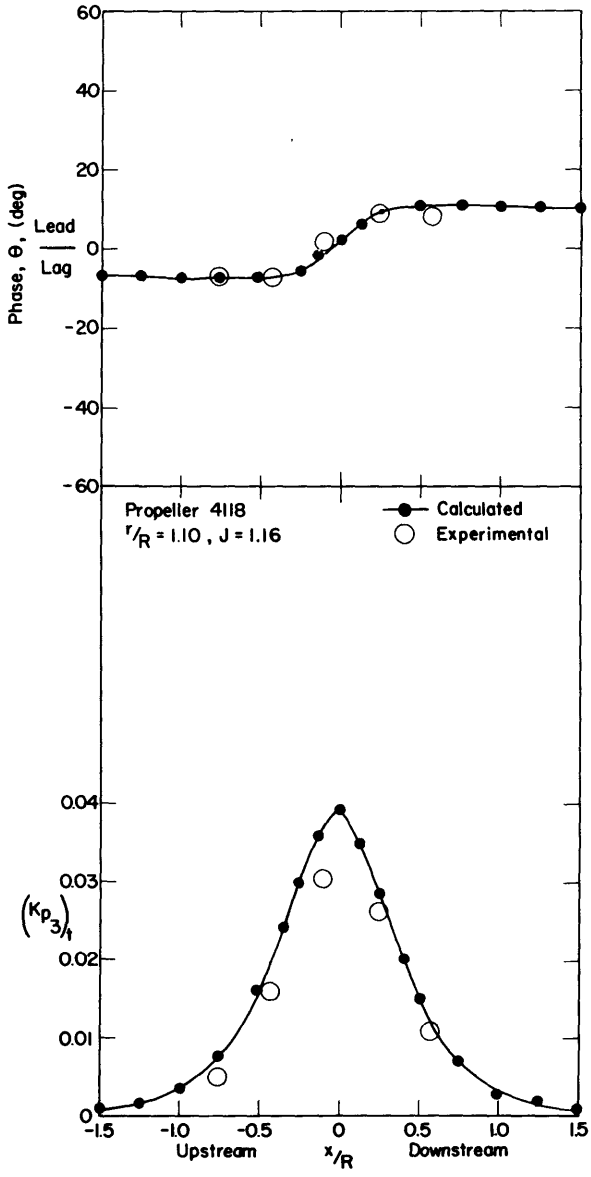

Figure 24 – Comparison of the Predictions of Kerwin's Method and Experimental Values, Thickness Contribution, r/R = 1.10, J = 1.16

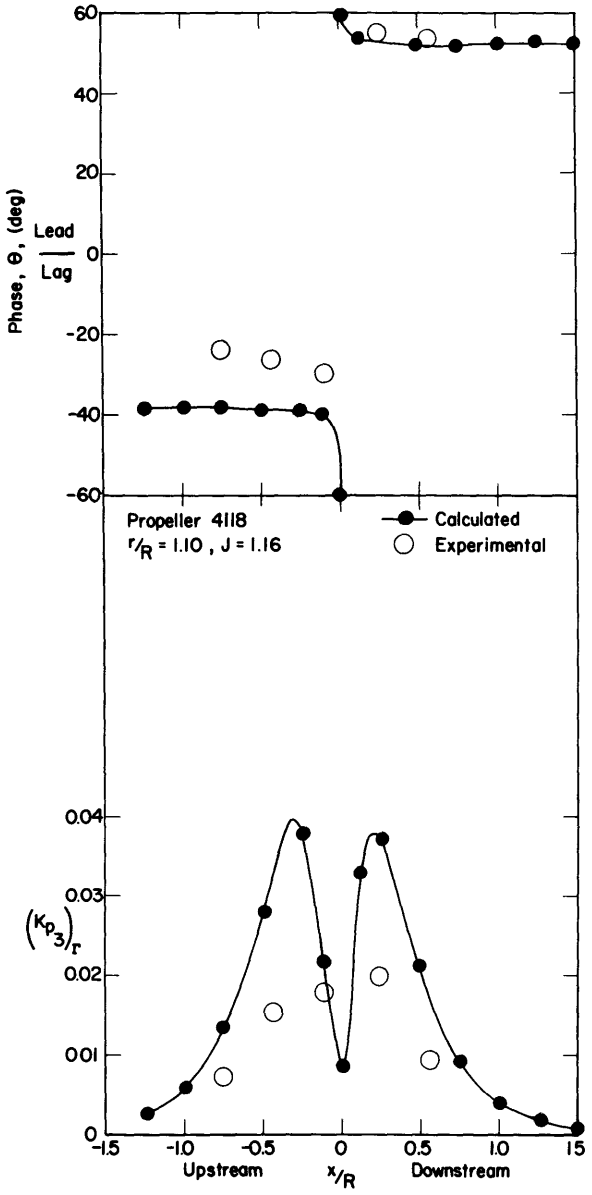

Figure 25 – Comparison of the Predictions of Kerwin's Method and Experimental Values, Loading Contribution, r/R = 1.10, J = 1.16

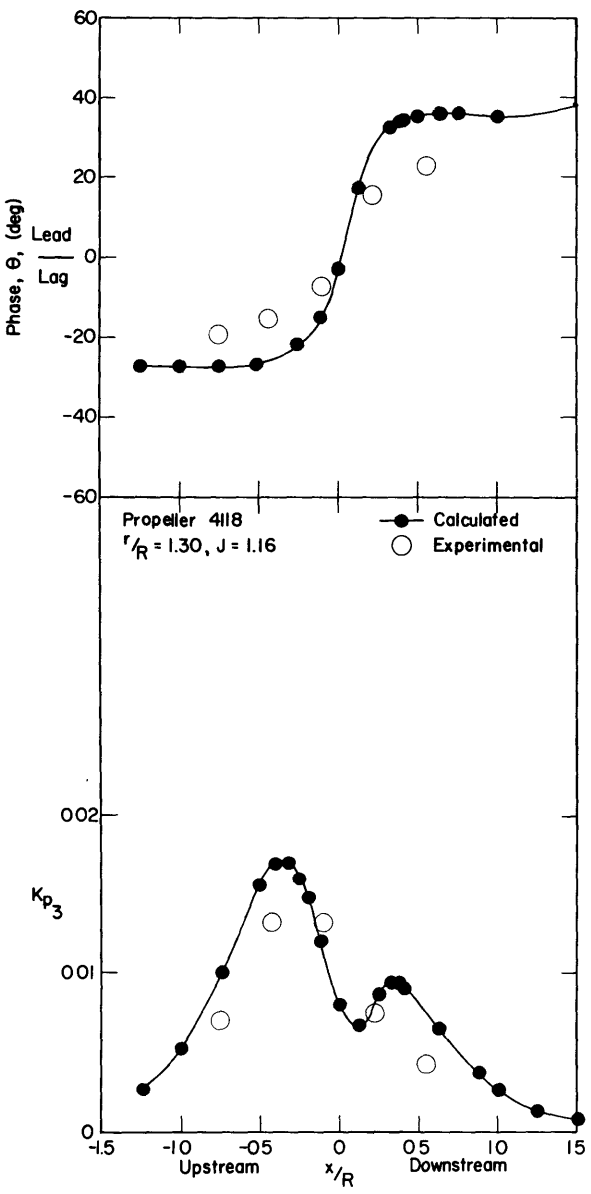

Figure 26 – Comparison of the Predictions of Kerwin's Method and Experimental Values, Total Blade-Rate Signal, r/R = 1.30, J = 1.16

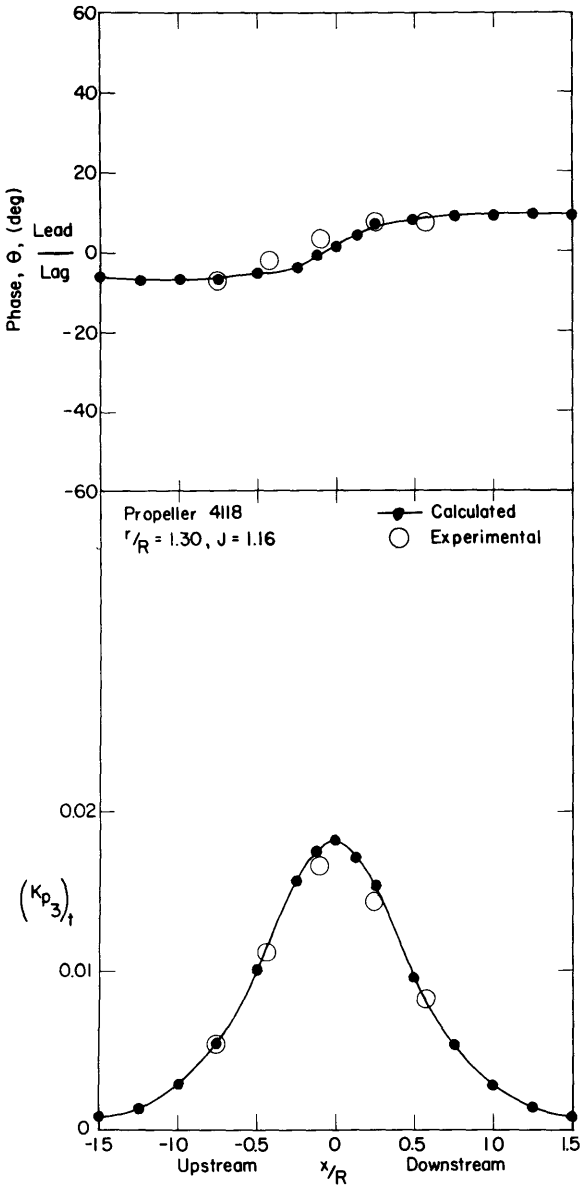

Figure 27 – Comparison of the Predictions of Kerwin's Method and Experimental Values, Thickness Contribution, r/R = 1.30, J = 1.16

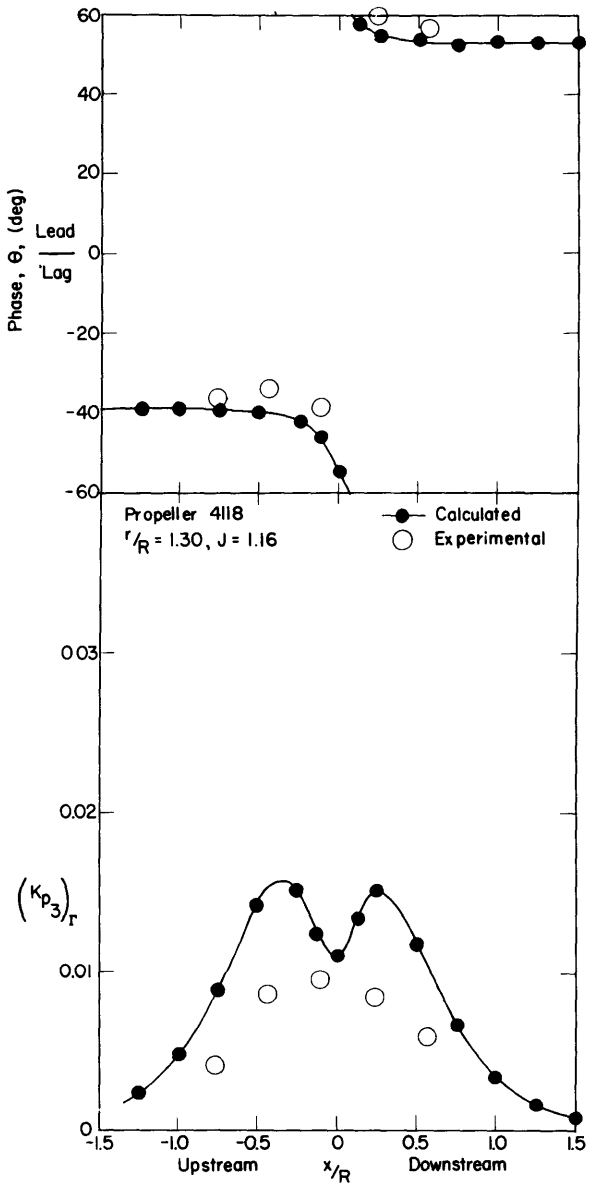

Figure 28 – Comparison of the Predictions of Kerwin's Method and Experimental Values, Loading Contribution, r/R = 1.30, J = 1.16

obtained by calculating for each propeller blade section a lift, the resolution of which, in the thrust direction, would be sufficient to counteract the component of drag in the negative-thrust direction. Two sets of results, using the lift-dependent circulation from the foregoing calculations and the corresponding induced axial velocities, were obtained with Kerwin's program. One set assumed NACA $a = 0.8$ mean lines and the other set assumed noncambered sections. All other input was identical. Blade-rate pressure results of the latter were subtracted, in phase, from those of the former and, in this manner, the angle of attack was effectively subtracted out and the drag was distributed over the blade surface.

Again the agreement between the calculated and the experimentally determined thickness contributions was very good. Prediction of amplitudes and phases of the loading signals was fair and equally as good as for the design advance and heavily loaded cases.

ADDITIONAL EXPERIMENTAL MEASUREMENTS

Cavitation Effects

At the conclusion of the comparisons between theory and experiment, additional pressure measurements were made showing the effect of propeller blade cavitation; two examples are presented here. Figure 29 shows the induced blade-rate amplitudes obtained at a plate clearance of 10 percent of the radius. Propeller 4118 was operating at the heavily loaded condition, $J = 0.60$, set by a thrust identity before the tunnel pressure was reduced. At $\sigma = 4.95$, sheet cavitation existed on the back of the propeller blades from the 40-percent radius to the tip. The measured results for noncavitating Propellers 4118 and 4119 at the same advance and tip clearance are superposed onto the plot. The first upstream transducer was inoperative during this cavitation test and no data at that location was obtained.

Figure 30 shows the measurements obtained at a plate clearance of 30 percent of the radius and at $\sigma = 17.0$. Sheet cavitation was present on the back of the blades from the 80-percent radius to the tip and noticeable tip vortices extended downstream.

Effects of Nonuniform Inflow

To generate an axial nonuniform inflow, the screen in Figure 31 was constructed and mounted 15 inches upstream of Propeller 4118. The screen produced a circumferentially varying sinusoidal wake of period $2\pi/3$. The harmonic analysis of the wake survey taken in the plane of the propeller is shown in Figure 32. The amplitudes of the third and sixth harmonics are represented as fractions of the volume mean flow velocity; all higher harmonics were less than 15 percent of the third harmonic. The phases ϕ_η represent the measured shift of the maximum downstream wake velocity from an alinement with the center of the high velocity region of the screen. Pressure measurements were taken at a plate clearance of 10 percent of the radius. The three advance conditions, in Figures 33, 34, and 35, are comparable to those of the uniform flow conditions and were established by setting the mean

(Text continued on page 34.)

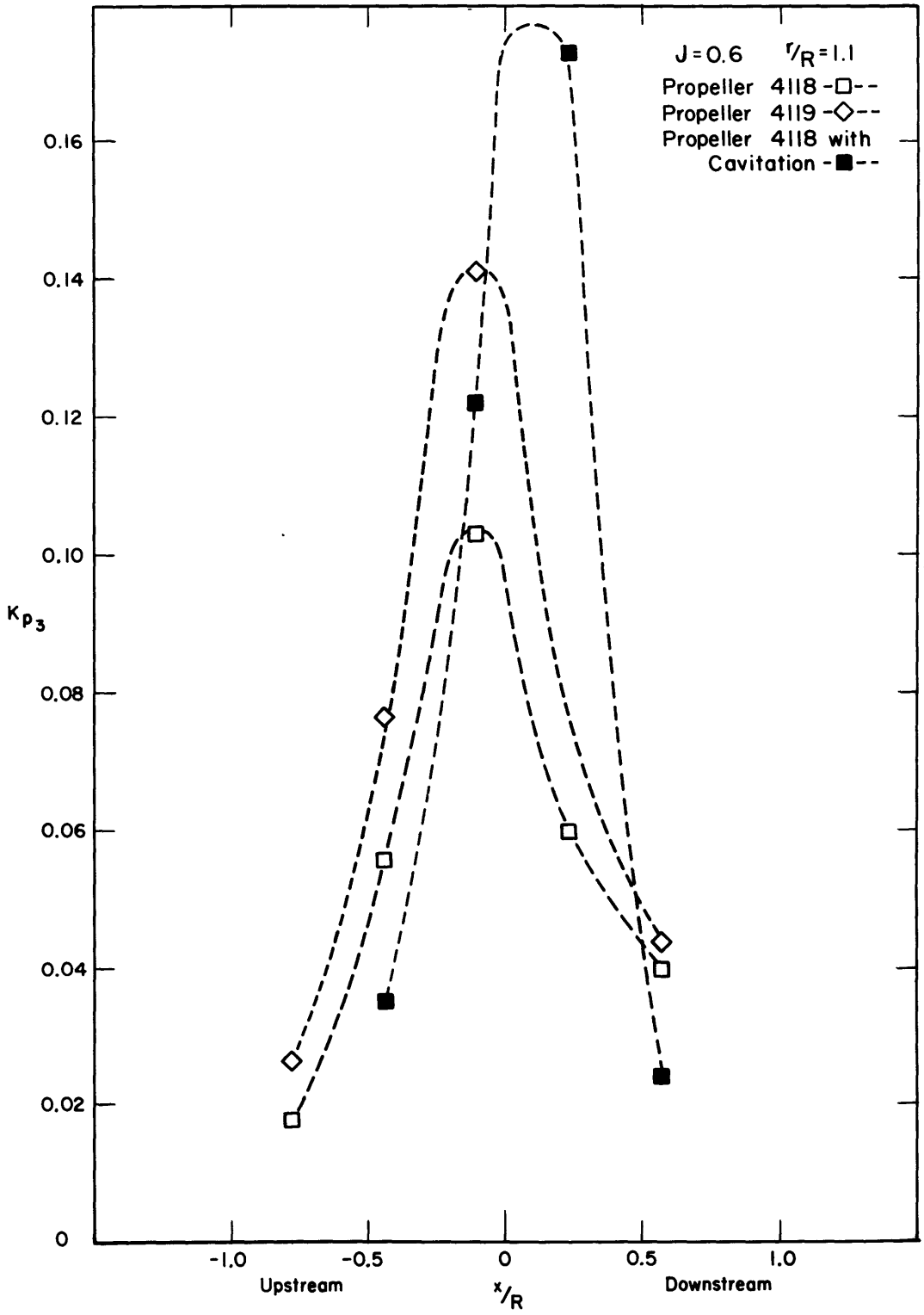

Figure 29 – Effect of Propeller Cavitation on Blade-Rate Pressures, r/R = 1.10

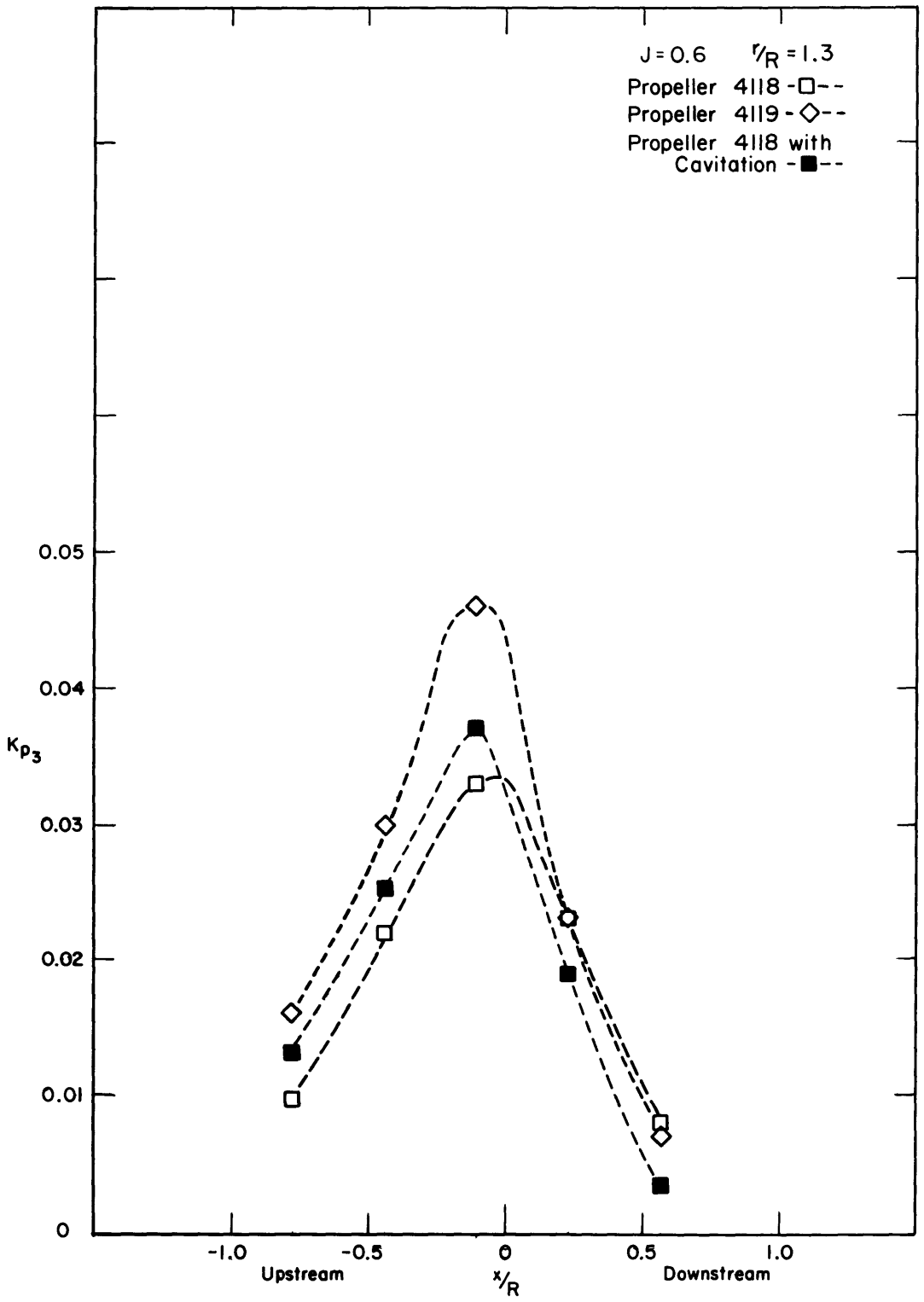

Figure 30 – Effect of Propeller Cavitation on Blade-Rate Pressures, r/R = 1.30

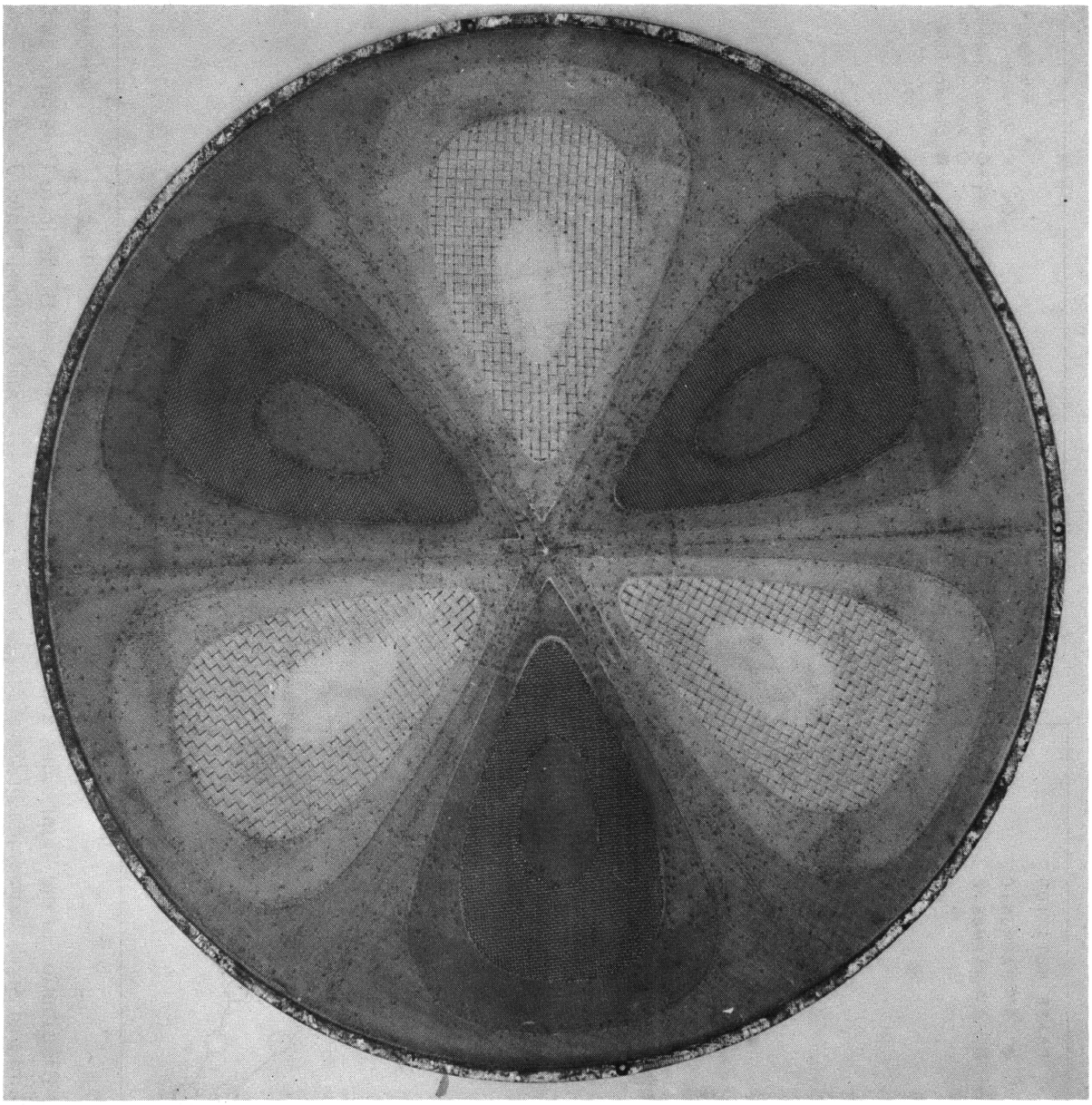

Figure 31 – Wake Screen Used in Nonuniform Inflow Experiments

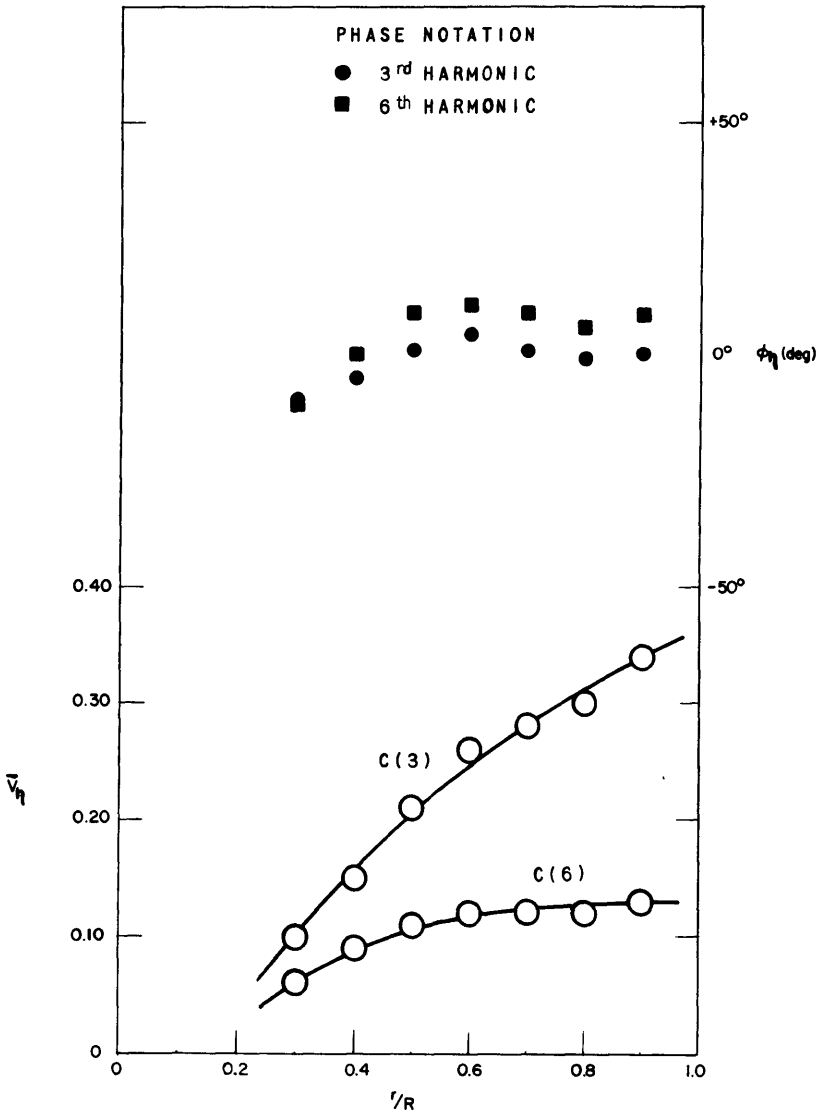

Figure 32 – Radial Distribution of the Amplitudes and Phases of the Third and Sixth Harmonics of the Circumferential Wake Variation

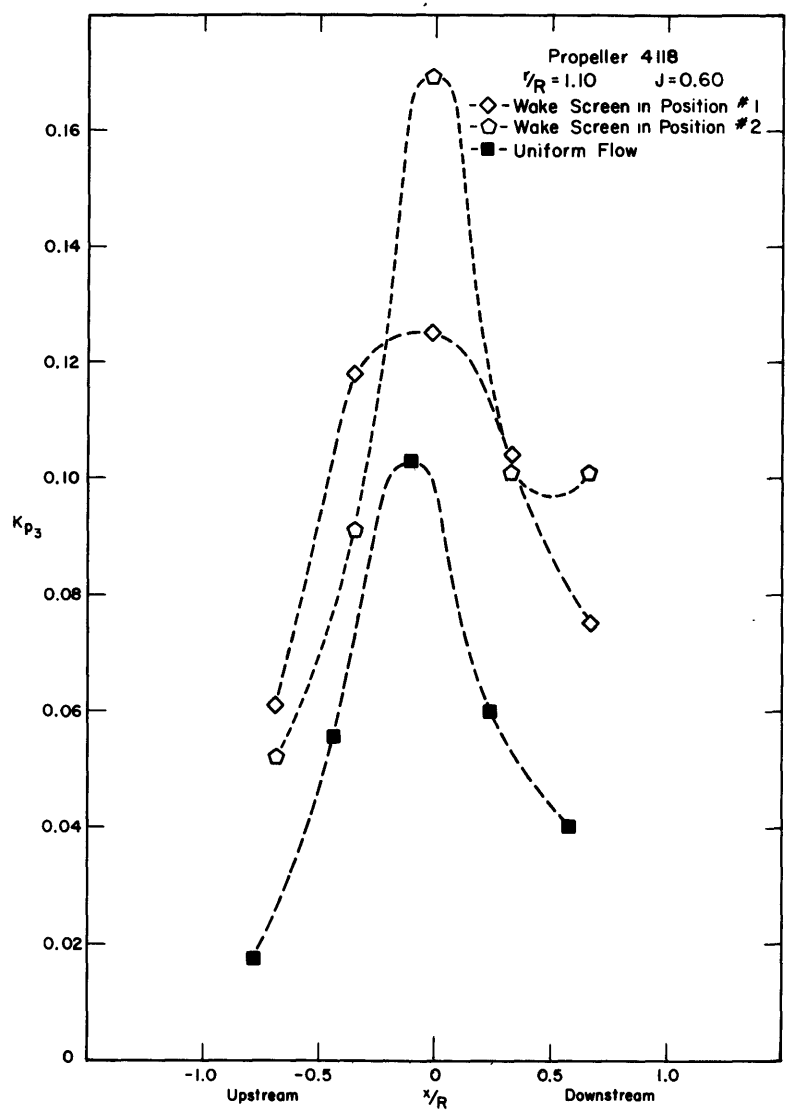

Figure 33 – Induced Blade-Rate Pressures in Nonuniform and Uniform Flow, $J = 0.60$

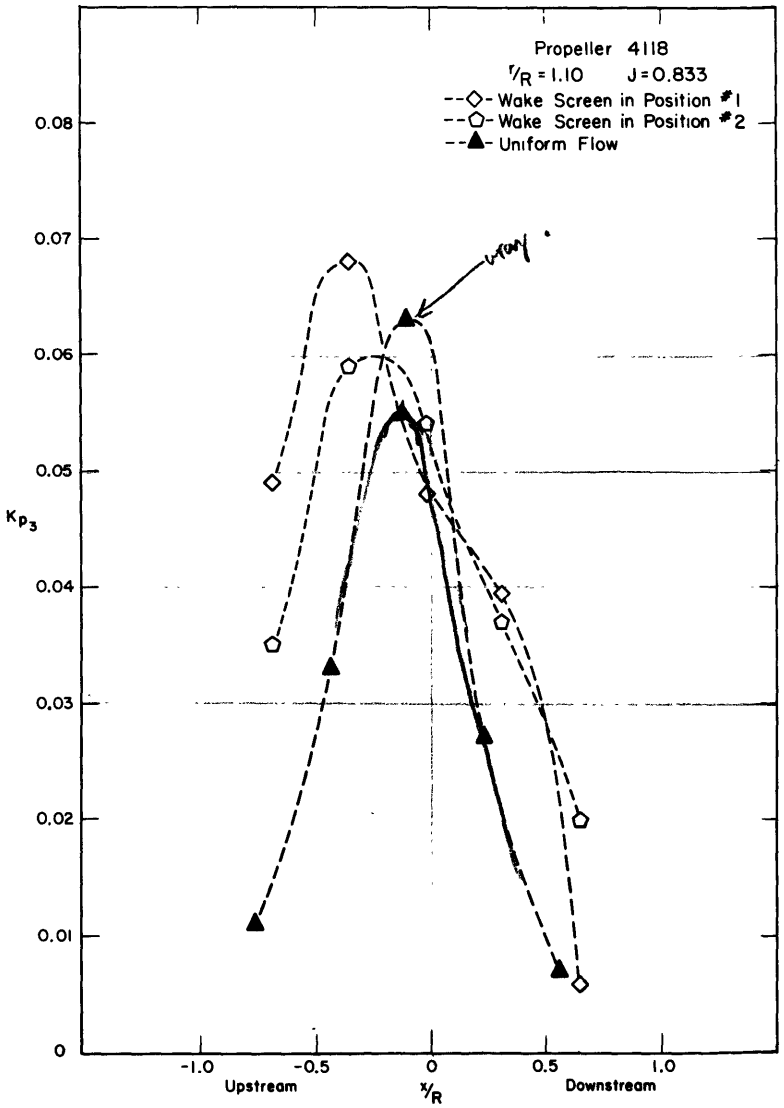

Figure 34 – Induced Blade-Rate Pressures in Nonuniform and Uniform Flow, J = 0.833

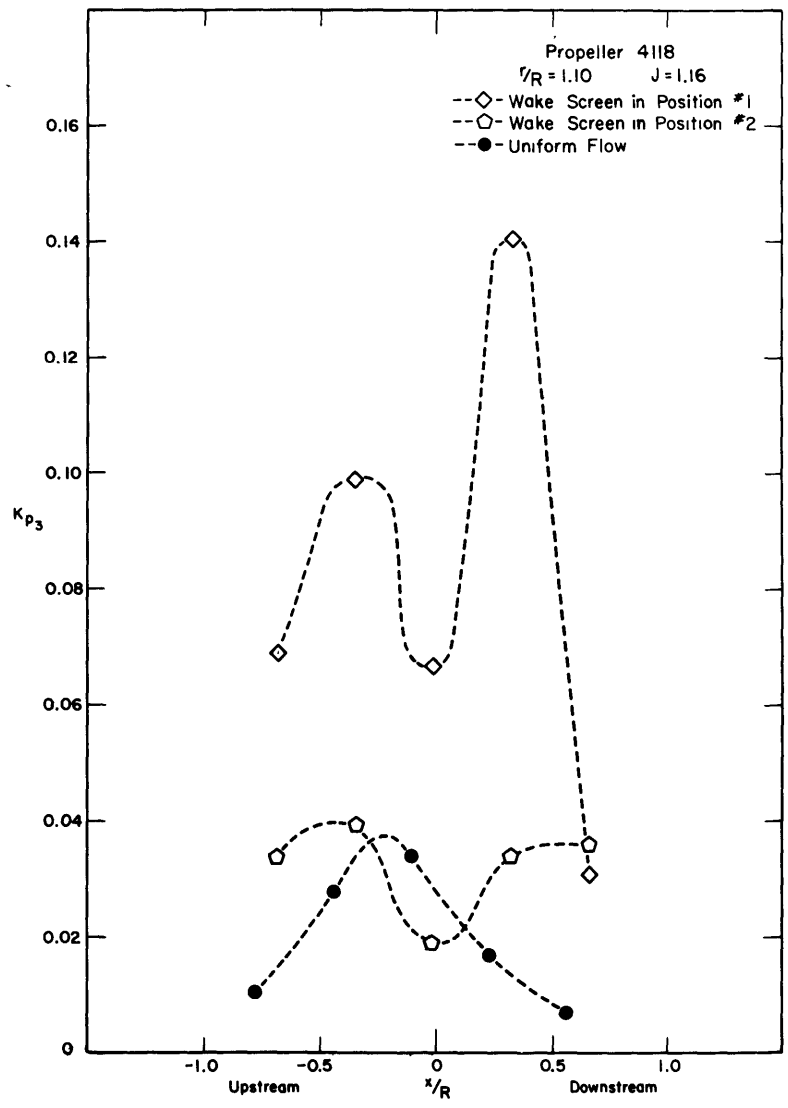

Figure 35 – Induced Blade-Rate Pressures in Nonuniform and Uniform Flow, J = 1.160

value of the thrust equal to that of a uniform flow case. Each plot shows the pressure measurement obtained at two rotative positions of the screen. The designation "Position No. 1" indicates results obtained while the center of the higher velocity region of the screen was nearest the plate. In Position No. 2 the lower velocity region was nearest the plate. Also shown on each plot are the measured pressures obtained during the corresponding operating condition in uniform flow.

Propeller Geometry Effects

To investigate the effects of certain propeller geometry parameters on induced field pressures, five propellers were chosen that were relatively different in construction but were designed to deliver identical thrust at the design advance coefficient, $J = 0.474$. The propellers were either 6- or 7-bladed and had an 11.52-inch diameter. Design information and drawings of the propellers, numbered 4060 through 4064, are presented in Figures 36 and 37.

Figure 38 shows the total pressure measurement results on the flat plate at a clearance of 15 percent of the propeller radius and with the propellers operating at design thrust. Phases and amplitudes are presented with separate plots depicting the blade-rate amplitudes of the 6- and 7-bladed propellers.

Since no pitch corrections to account for blade thickness had been included in the design of this propeller series, performance did vary and at design thrust the advance coefficient J ranged from 0.39 to 0.48.

Figure 39 shows the axial variation in pressure phases and amplitudes obtained while the propellers were operating at the zero-thrust condition, $0.6 < J < 0.7$. The results in the plots, at both conditions, show similar trends. It is obvious that the extreme skew of Propeller 4063 and the increased blade area of Propeller 4064 reduce the total blade-rate pressure signal. No significant reduction is noted in the signal of moderately skewed Propeller 4061, and also, no appreciable differences are visible between the blade-rate signals of 6-bladed Propeller 4060 and 7-bladed Propeller 4062.

CONCLUSIONS

Close agreement between the predictions of the induced pressures due to propeller thickness by both methods, Kerwin's and Breslin's, and the excellent agreement between these predictions and the experimental results indicate that field pressure thickness effects can now be accurately calculated. Also, it follows, at least in the example presented here, that the approximation, that the thickness contribution to field pressures could be considered linear, was a valid assumption. The experimentally determined thickness contributions agreed well in amplitude comparisons and fairly well in phase comparisons with the predictions of Kerwin's method at all three advance conditions and with the predictions of Breslin's method at design advance.

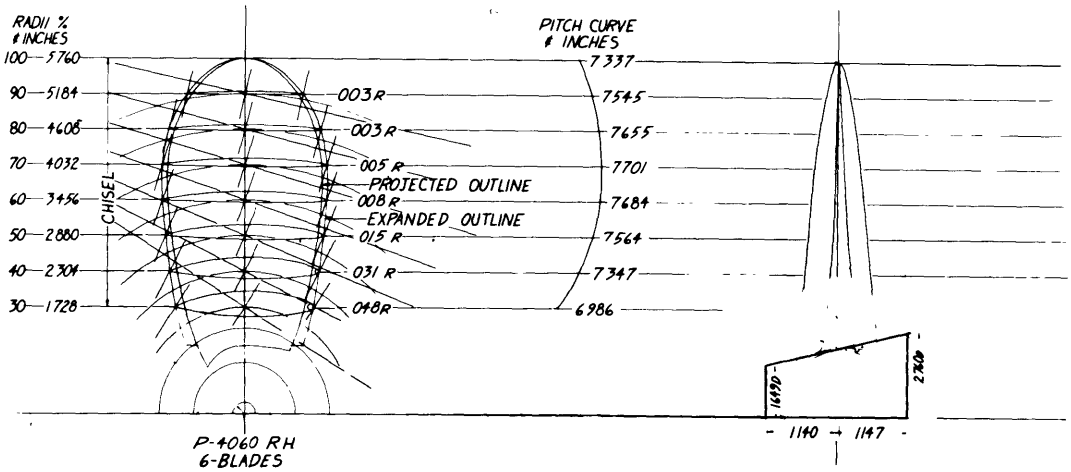

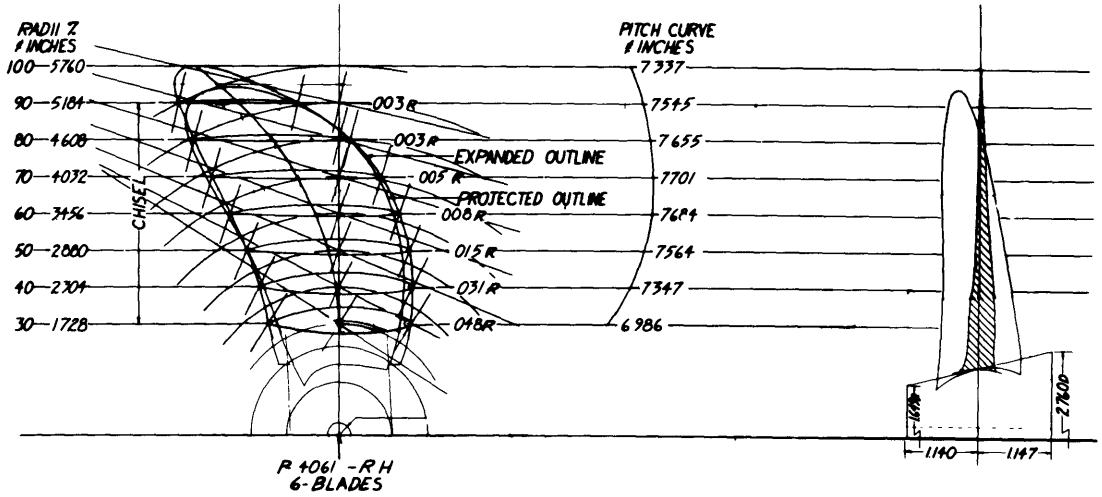

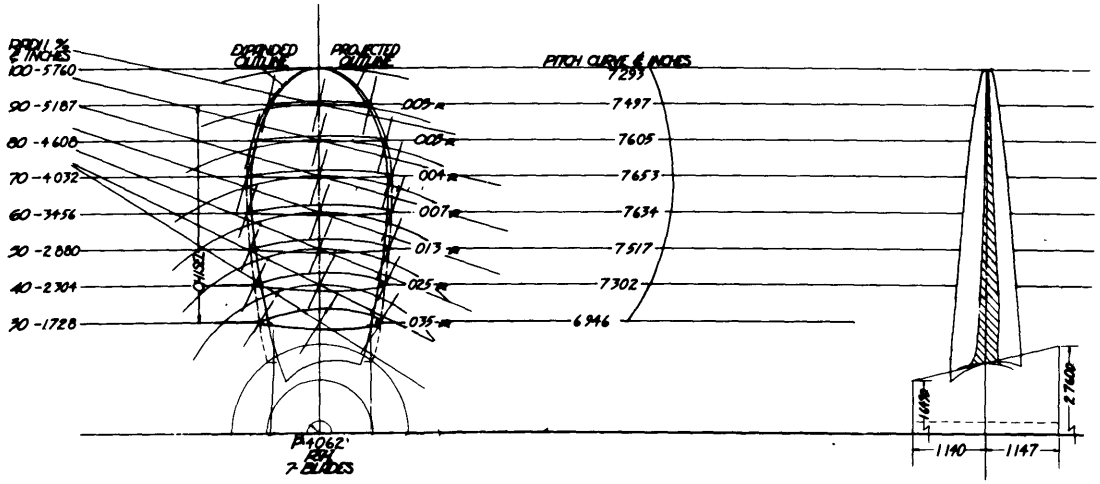

Figure 36 – Drawings and Design Information, Propellers 4060-4064

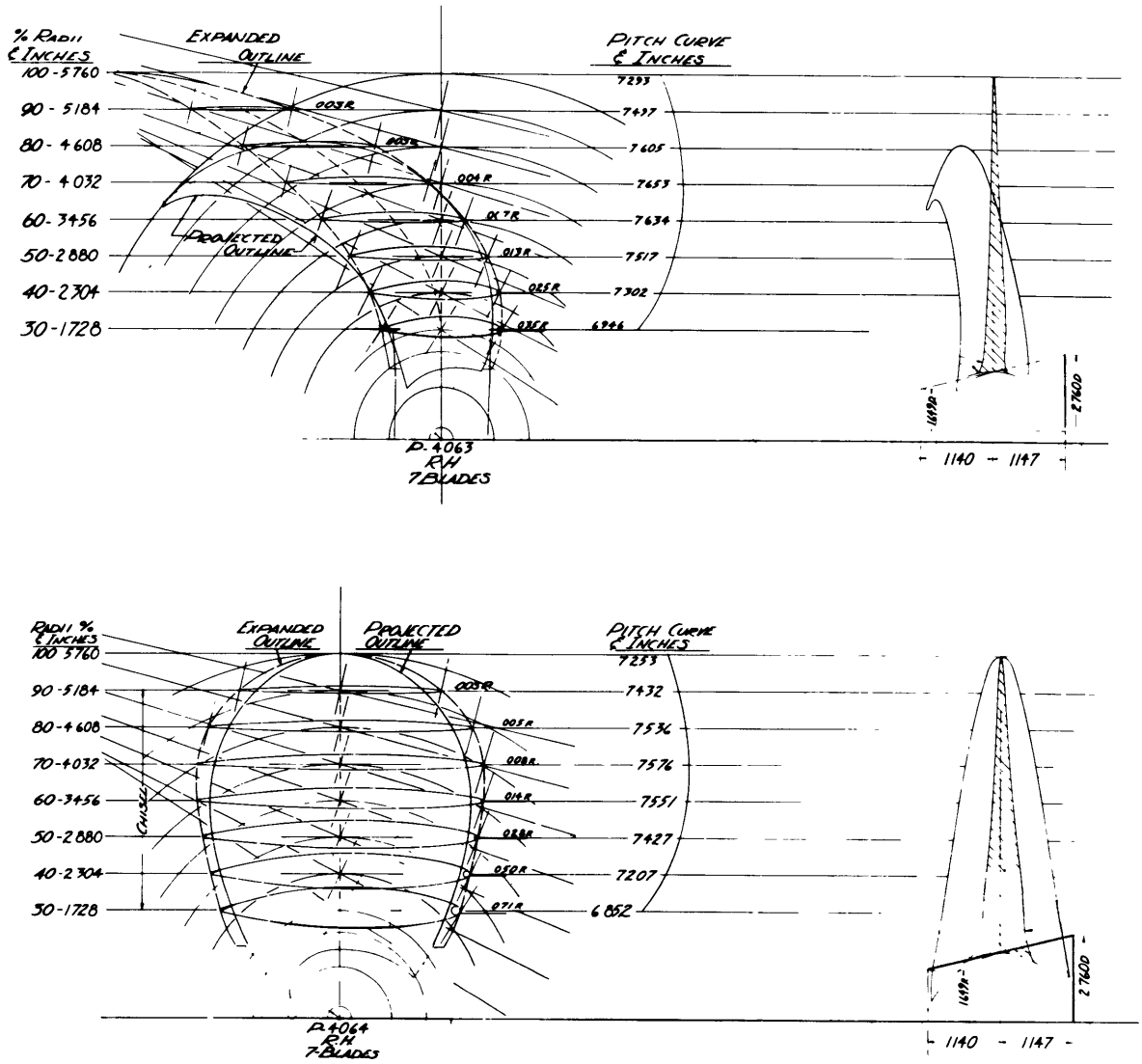

Propeller	Number of Blades	E. A. R.	Skew
4060	6	0.60	None
4061	6	0.60	Moderate
4062	7	0.60	None
4063	7	0.60	Extreme
4064	7	1.20	None

Design K_T = 0.11

Design J = 0.474

Figure 37 – Drawings and Design Information, Propellers 4060-4064

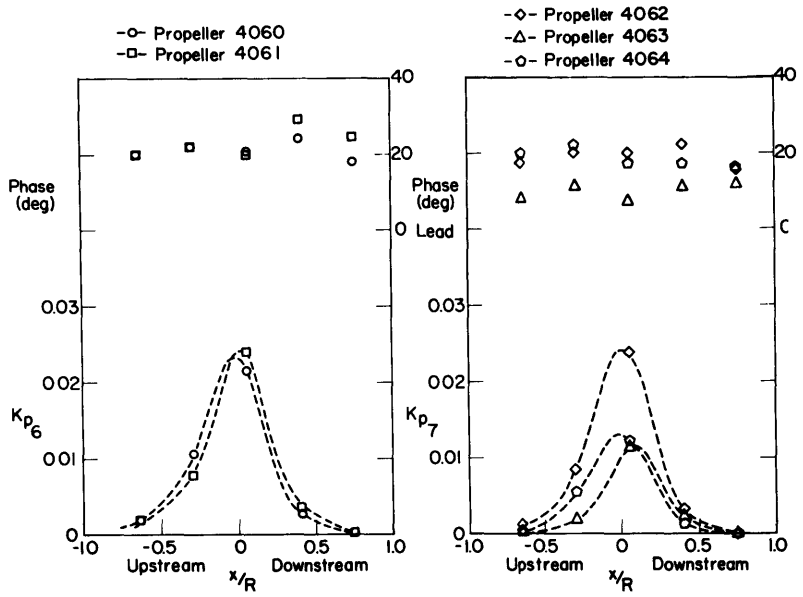

Propeller	Number of Blades	E. A. R.	Skew
4060	6	0.60	None
4061	6	0.60	Moderate
4062	7	0.60	None
4063	7	0.60	Extreme
4064	7	1.20	None

Figure 38 – Blade-Rate Pressures, Design Thrust, r/R = 1.15

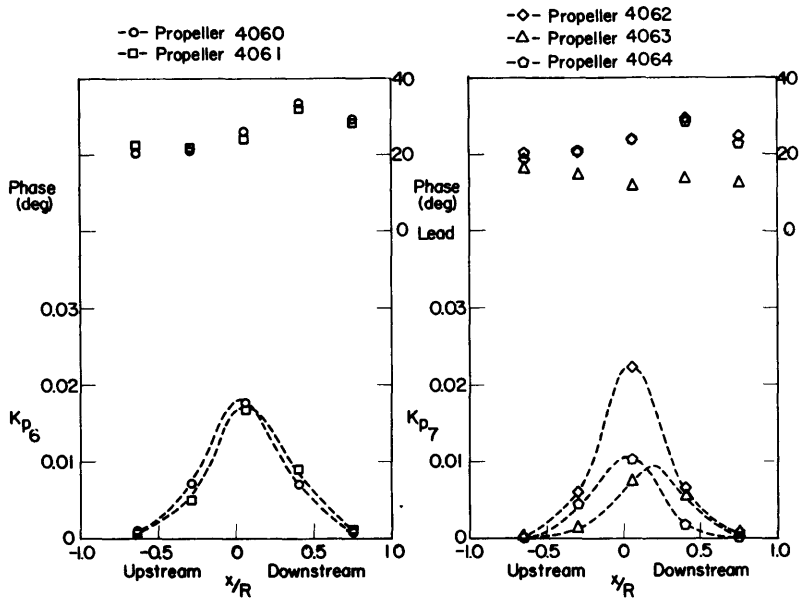

Propeller	Number of Blades	E. A. R.	Skew
4060	6	0.60	None
4061	6	0.60	Moderate
4062	7	0.60	None
4063	7	0.60	Extreme
4064	7	1.20	None

Figure 39 – Blade-Rate Pressures, Zero Thrust, r/R = 1.15

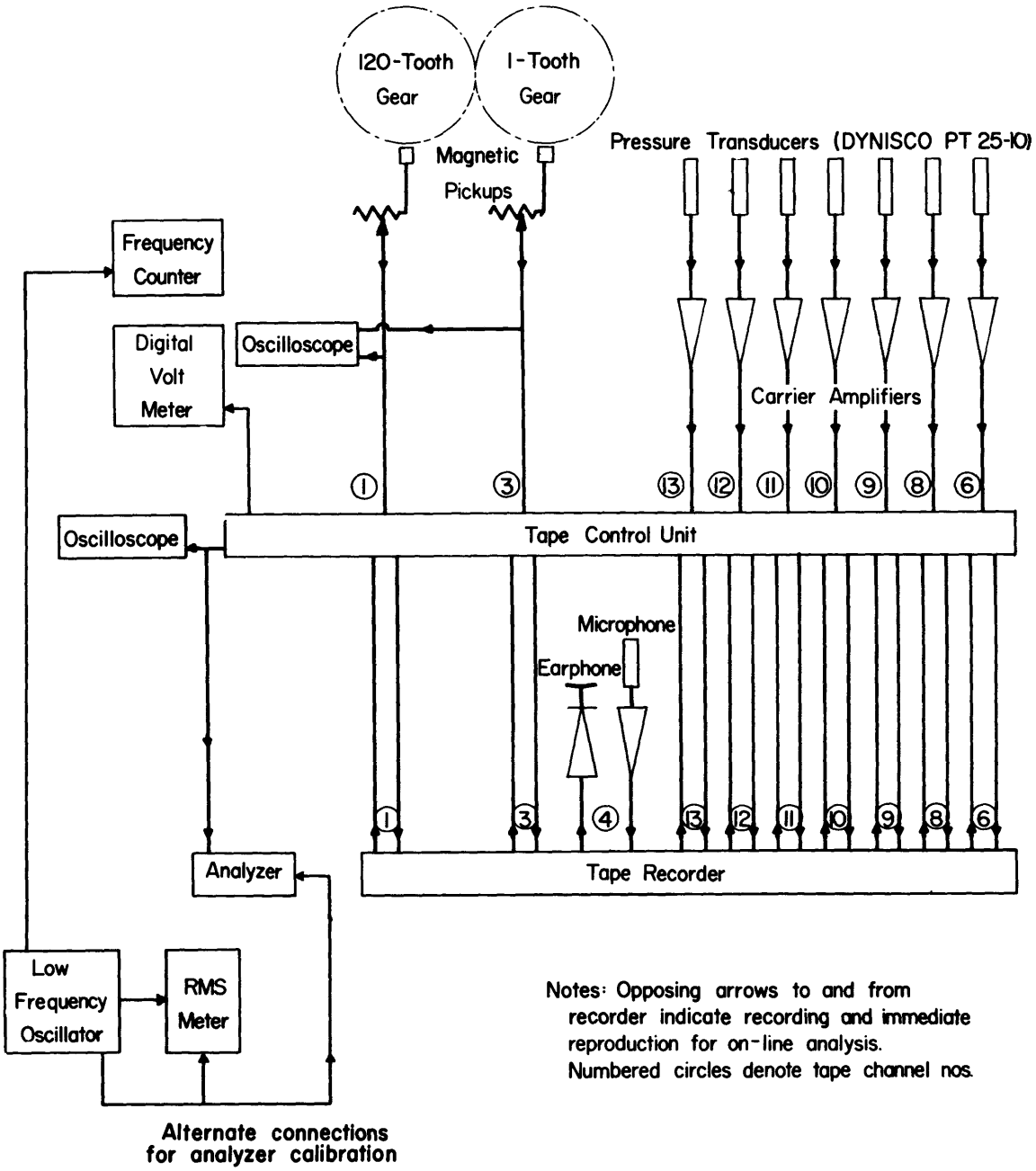

Figure 40 – Block Diagram of Electronic Instrumentation

At design advance, comparisons with theory were made at the 10-percent and 30-percent propeller radius plate clearance. For the 10-percent clearance, calculated loading amplitudes tended to be higher than those experimentally found to exist and particularly so downstream of the propeller. The phase predictions from Kerwin's method were very good, whereas the phase results of Breslin's method did not agree well with the experimental results and were very poor downstream. At the 30-percent radius clearance, loading amplitudes calculated with Kerwin's method again were larger than the experimental results, but the phase agreement was excellent.

Comparisons for the off-design advance condition, which were made only between the Kerwin method calculations and experimental results, showed slight discrepancies in the phase results. Pressure amplitude predictions, however, approximated the experimental results as well as in the design advance cases.

The nondiminishing feature of the predicted downstream pressure amplitudes from Kerwin's method, present in the loading comparisons, was a subject of much investigation. It was decided that the phenomenon was not the fault of an incorrect numerical evaluation of the downstream velocity functions. Nor was it entirely the fault of neglecting the contraction and elongation of the downstream trailing vortices.

Certainly there is always an honest doubt about the reliability of results obtained from experiments. However, in this case, it was felt that water speeds were sufficiently high to force the boundary layer buildup on the plate to be negligible; and even if it were not, an increased loading of the propeller blades would be imposed near the plate and blade-rate pressures would be increased rather than reduced.

It is suggested that the possible roll-up of the downstream vortices, or the intricate character of the vortices, if roll-up is not the answer, is such that no present mathematical model can accurately describe their effects on induced field velocities. Undoubtedly, more experimental information is needed on downstream induced velocities both within and outside of the propeller race and for a variety of loadings.

Comparative calculations derived by Breslin's theory were limited to one case in this work. In spite of the method's poor prediction of phase, it does offer a handy simple procedure for calculating blade-rate pressure amplitudes induced by lightly loaded propellers. The work presented here was initiated to check the reliability of Kerwin's method, which is definitely a more thorough numerical procedure and, as proven here, is quite versatile in investigations of induced pressure effects of propellers at off-design conditions.

From the purely experimental results, it was obvious that propeller blade cavitation considerably increases the induced field pressures. Since the cavitation runs were limited in number, no attempt was made to correlate the pressure increase to virtual increased blade thickness effects, although this approach is conceivable.

Extreme propeller blade skew and increased blade area proved to reduce considerably the field-point blade-rate pressure signals.

Nonuniform axial inflow to parent Propeller 4118 produced sizable variations in field pressures. The variations exhibited a strong dependence on the advance coefficient as well as the angular position with respect to the wake. Considerably more data was taken during the wake conditions and the analysis of that data is continuing.

Additional experimentation in pressure measurements near marine propellers is planned at DTMB for the near future. Many of the test conditions presented here will be closely duplicated in measurements to be made in the towing basin. In addition to obtaining more pressure information at different tip clearances and at distances farther upstream and downstream, the future measurements will provide a check of the measurements on the flat plate in the closed-jet experiments and will determine whether sufficient flow distortion was present on the flat plate to alter the measured data and violate the pure image assumption maintained in the analysis.

ACKNOWLEDGMENT

Credit is due Mr. Justin H. McCarthy for his planning, experimentation, and guidance in the analysis.

APPENDIX

Figure 40 is a block diagram of the equipment and circuitry involved in the oscillating pressure measurements. The single and 120-toothed gears were located on the propeller shaft with the single magnetic signal recorded directly on tape and 120 pulses per revolution used to trigger simultaneous pressure recording of the signals from all transducers.

Descriptive information on the components of the apparatus follows:

1. The pressure transducers were Dynisco PT25-10. They are high frequency response transducers, of the strain gage-diaphragm type, effective in the range of 0-10 psi, gage or absolute. The transducers have a minimum output of 4 mv/v and an excitation of 6 v ac or dc.

2. Signals were amplified by Sanborn Carrier Amplifiers. The amplifiers, Model No. 350-1100, excited the transducers with a 6-v rms signal at 2400 Hz.

3. The tape control unit enabled direct recording of transducer fluctuating signals and d-c calibration signals. Inherent in the control system was the ability to monitor, one at a time, the input or output of the individual recorder channels.

4. Recording was accomplished with a 14-channel Precision Instrument tape recorder, Model PS-200A. Voice and gear tooth channels were recorded directly and all data were recorded with FM at 15 ips and with a frequency response of dc to 10 kHz. Maximum input was ± 1.41 v dc.

5. On-line analysis was made with a combined General Radio Analyzer (1564-A) and a General Radio Graphic Level Recorder (1521A). Signal amplitudes were obtainable at desired frequencies.

All tape data digitization and harmonic analysis were carried out at the Applied Mathematics Laboratory of the David Taylor Model Basin.

REFERENCES

1. Tachmindji, A.J. and Dickerson, M.C., "The Measurement of Oscillating Pressures in the Vicinity of Propellers," David Taylor Model Basin Report 1130 (Apr 1957).

2. Pohl, K.H., "Die durch eine Schiffschraube auf benachbarten Platten erzeugten periodischen hydrodynamischen Drucke," Schiffstechnik, 35 Heft, 7 Band (Feb 1960).

3. Pohl, K.H., "Das instationare Druckfeld in der Umbebung eines Schiffspropellers und die von ihm auf benachbarten Platten erzeugten periodischen Krafte," Schiffstechnik, 30-34 Heft, 6 Band (1959).

4. Kowalski, T. and Breslin, J.P., "Experimental Study of Propeller-Induced Vibratory Pressures on Simple Surfaces and Correlation with Theoretical Predictions," Davidson Laboratory Report No. 973 (Jul 1963).

5. Kerwin, J.E., "A Design Theory for Subcavitating Propellers," Transactions of Society of Naval Architects and Marine Engineers, Vol. 72 (1964).

6. McCarthy, J.H., "A Method of Wake Production in Water Tunnels," David Taylor Model Basin Report 1785 (Oct 1963).

7. Lerbs, H.W., "Moderately Loaded Propellers with a Finite Number of Blades and an Arbitrary Distribution of Circulation," Transactions of the Society of Naval Architects and Marine Engineers, Vol. 60 (1952), pp. 73-117.

8. Borst, H.W., et al., "A Theory for VTOL Propeller Operation in a Static Condition," a joint report by Curtiss-Wright Corporation and Therm Advanced Research, Inc. (May 1965).

9. Kerwin, J.E., "Propeller Field Point Velocities," Massachusetts Institute of Technology Report (in preparation).

10. Breslin, J.P., "The Pressure Field Near a Ship Propeller," Journal of Ship Research, Vol. 1, No. 4 (Mar 1958).

11. Breslin, J.P. and Tsakonas, S., "Marine Propeller Pressure Field due to Loading and Thickness Effects," Transactions of Society of Naval Architects and Marine Engineers, Vol. 67, No. 6 (1959).

INITIAL DISTRIBUTION

Copies

- 3 NAVSHIPSYSCOM
  - 3 Scientific Documentation Br (Ships 2021)
- 8 NAVSEC
  - 2 Ship Concept Design Div (Sec 6360)
  - 1 Ship Sys Engin & Des Dept (Sec 6100)
  - 1 Propulsion, Power & Auxiliary Sys Div (Sec 6140)
  - 2 Propulsion Sys Analysis Br (Sec 6144)
  - 2 Prop Shaft & Brng (Sec 6148)
- 1 NAVMAT (MAT 0331)
- 2 NAVAIRSYSCOM
  - 2 AIR 604
- 3 CHONR
  - 2 Fluid Dynamics Br (Code 438)
  - 1 Sys & Res Gp (Code 492)
- 1 DIR, USNOTS, Pasadena
- 1 CO & DIR, USNMEL
- 1 CDR, USNOL
- 1 DIR, USNRL
- 1 NAVSHIPLO, APO New York
  - Attn: Mr. A.C. Kloske
- 20 CDR, DDC
- 1 NASA, Manned Flight Projects
  - Attn: Dr. W.L. Haberman
- 3 MARAD
  - 2 Administrator
  - 1 Mr. Kenneth A. Myers
- 1 CIT, Hydro Lab, Pasadena
- 2 ORL, Penn State
  - 1 Director
  - 1 Dr. Maurice Sevik
- 2 NAME, MIT
  - 1 Head of Department
  - 1 Prof. Frank M. Lewis
- 1 DIR, Iowa Inst of Hydraulic Res

Copies

- 2 Univ of Michigan, NAME
  - 1 Head of Department
  - 1 Dr. Finn C. Michelsen
- 3 Inst of Nav Arch, Webb Univ
  - 1 Administrator
  - 2 PGSCOL
- 1 Oceanics, Inc., New York
- 2 Univ of Calif, Berkeley
  - 1 Attn: Librarian
  - 1 Attn: Head, Dept of NAVARCH
- 1 Gibbs and Cox, Inc., New York
- 1 George G. Sharp, Inc.
- 1 Grumman Aircraft Corp.
- 1 Hydronautics, Inc.
- 1 Aerojet-General Corp., Azusa
- 1 Martin Company, Baltimore
- 1 Boeing Aircraft Corp.
- 1 United Aircraft Corp., Hamilton Standard Div., Conn.
  - Attn: Mr. G. Rosen
- 1 Kamen Aircraft Corp
- 1 SNAME
- 1 ASNE, Inc., Washington, D.C.
- 1 Applied Mechanics Reviews, Southwest Res Inst, San Antonio 6, Texas
- 1 Engineering Index, Inc., New York, New York
- 1 Puget Sound Bridge and Drydock Co., Seattle, Washington
- 1 ONR, Boston
- 1 ONR, Pasadena
- 1 ONR, Chicago
- 1 ONR, New York

Copies

1 ONR, London

1 ONR, San Francisco

1 Bethlehem Steel Company

1 Douglas Aircraft Company

1 GASL, Inc., New York

1 Inst of Aerospace Sciences, Inc., New York
Attn: Librarian

1 ITEK Corp., Vidya Div, Palo Alto, California

1 NNS & DDC, Engineering Tech Dept

1 TRG, Inc., Milville, New York

1 DIR, St. Anthony Falls Hydraulic Lab, Univ of Minnesota, Minneapolis, Minnesota

1 Univ of Notre Dame, Dept of Eng Mech

1 Therm, Inc.

1 Lockheed, Sunnyvale, California
Attn: Dr. Cuthbert

1 IDA

3 SIT, Davidson Lab
2 Dr. John P. Breslin
1 Mr. Charles J. Henry

UNCLASSIFIED

Security Classification

DOCUMENT CONTROL DATA - R & D

(Security classification of title, body of abstract and indexing annotation must be entered when the overall report is classified)

1 ORIGINATING ACTIVITY *(Corporate author)*

Naval Ship Research and Development Center
Washington, D.C. 20007

2a. REPORT SECURITY CLASSIFICATION

Unclassified

2b. GROUP

3 REPORT TITLE

COMPARISONS OF EXPERIMENTALLY DETERMINED AND THEORETICALLY PREDICTED PRESSURES IN THE VICINITY OF A MARINE PROPELLER

4 DESCRIPTIVE NOTES *(Type of report and inclusive dates)*

Final report

5 AUTHOR(S) *(First name, middle initial, last name)*

Denny, Stephen B.

6 REPORT DATE	7a. TOTAL NO OF PAGES	7b. NO OF REFS
May 1967	51	11

8a. CONTRACT OR GRANT NO	9a. ORIGINATOR'S REPORT NUMBER(S)
b. PROJECT NO Z-R011 01 01	2349
c. Problem Number 526-356	9b. OTHER REPORT NO(S) *(Any other numbers that may be assigned this report)*
d.	

10 DISTRIBUTION STATEMENT

Distribution of this document is unlimited.

11 SUPPLEMENTARY NOTES	12 SPONSORING MILITARY ACTIVITY
	Naval Ship Systems Command Washington, D.C. 20360

13 ABSTRACT

Pressures were measured on a flat plate placed near a model marine propeller in the 24-inch water tunnel at the David Taylor Model Basin. The blade-rate portions of the values measured in uniform flow are compared with field-point pressure predictions of theories for two propeller tip clearances and three advance conditions. Also shown are comparisons between theory and experiment of the separate contributions of propeller thickness and loading.

Additional experimental results show the effect of blade number, blade area ratio, and blade skew on propeller-induced pressures. Flat-plate pressure measurements were also obtained near a propeller operating in nonuniform flow and at a cavitating condition in uniform flow.

The two theories investigated, field-point pressure calculation methods by Kerwin and by Breslin, both gave good predictions of the magnitudes of the induced blade-rate pressures due to blade thickness. The experimentally determined blade-rate pressures due to loading and the consequent total pressures, however, tended to be lower than the theoretical predictions downstream of the propeller. Breslin's theory gave predictions of pressure phase which were poor for the entire experimental region, whereas the predictions of Kerwin's method were good except in the aforementioned downstream area.

From the experiments it was found that a considerable reduction in induced blade-rate pressure results from increased blade area and extreme blade skew. Propeller blade cavitation increased the induced field pressures. Pressures induced by the propeller while it operated in nonuniform flow tended to be considerably larger than those induced during a corresponding advance in uniform flow and particularly so at off-design advance conditions.

14 KEY WORDS	LINK A		LINK B		LINK C	
	ROLE	WT	ROLE	WT	ROLE	WT
Propeller-Induced Field Pressures						